Tunable diode laser frequency stabilization and its applications in temperature measurement

Master in Science

by

Ali Rabbani

Supervisors:

Zhongshan Li

Jesper Borggren

Combustion physics

Lund University

June 2015

Table of Contents

Contents

List of Figures

Abstract

The frequency of two external cavity diode lasers tuned to the two transitions at *410 nm* and *451 nm* of indium are stabilized in this thesis. A hollow cathode lamp of indium atoms is used as a low pressure source of indium atoms in the locking process. Two frequency stabilization methods, *wavelength modulation spectroscopy* (*WMS*) and *polarization spectroscopy* (*PS*), are used in the thesis for the laser locking. In both methods a computer generated sweeping current is sent to a diode laser to produce a wavelength scan around a resonant transition of indium. The laser passes through the lamp and recorded on a photodiode. The recorded signal will be transferred to a computer program. The program, in the case of wavelength modulation spectroscopy locking technique, reduces the scanning range in order to lock the laser to the transitions of indium atoms. The polarization spectroscopy locking program sets the diode laser frequency to the specified transition of indium atoms to lock the laser.

The frequency stabilized lasers are used to conduct temperature measurements in an indium seeded flame with two-line atomic fluorescence. A flow of nitrogen gas seeds trimethylindium molecules to the flame and the exothermic combustion processes in the flame breaks the trimethylindium molecule bonds to produce free indium atoms. Two line atomic fluorescence thermometry technique is used to measure the temperature of the flame. A thin sheet of a stabilized diode laser is used to excite indium atoms.

Frequency stabilization of the two lasers was done within *250 MHz* for *WMS* and *110 MHz* for *PS* allowing for high precision temperature measurements. The preliminary temperature measurements showed great potential for future measurements in combustion environments.

1. Introduction

Combustion is a high temperature exothermic chemical reaction which plays a major role in modern civilization. Combustion processes are used for energy conversion, heating, and manufacturing. Along with its every day uses, combustion, of especially fossil fuels, gives rise to some major concerns with regards to fuel availability, environmental impact, human health, and climate change.

Despite using combustion processes in many areas for thousands of years, these processes currently are not entirely well understood. Better understanding of the combustion reactions is necessary to increase the efficiency and cleanness.

Many of the limitations in understanding the combustion processes are caused by difficulties of probing them. These difficulties are caused by the processes' hostility, the high temperature environments and fast heat release by the exothermic chemical reactions. The delicacy of combustion reactions along with hostility of them causes more difficulty in probing the environments to the point that any physical intrusion of probing devices may easily alter them [1].

Advancement in lasers has opened up a new field for nonintrusive optical diagnostic methods in combustion environments. Pulsed lasers providing high temporal and spatial resolution have solved a myriad of problems related to the probing of flames. Many laser spectroscopic techniques have been developed and can be used to investigate the key characteristics of combustion processes, such as temperature, chemical composition, and the flow field.

This thesis consists of two parts. In the first part, a process of locking a tunable diode laser to a resonant frequency of indium atoms' transition is conducted. Two different methods for locking the laser are used: *wavelength modulation spectroscopy* and

polarization spectroscopy. Narrow linewidth laser has played a major role in precise measurements in many fields of science. For example, atomic clocks need a very stable laser to probe the sub-hertz linewidth of samples. Laser-cooling also needs a highly stable laser.

For laser frequency stabilization with *wavelength modulation spectroscopy*, higher harmonics and a fitting method are used to lock the laser to specific transitions of indium atoms. An indium hollow cathode lamp (*HCL*) is used as a source of indium atoms. A *LabVIEW* computer program generates the modulated signal in a specific range and uses a Fourier demodulation method to separate the first and second harmonics from the input signal. The program reduces the scanning range of the laser to a small interval around the resonant transition which will serve as a modulated frequency stabilization technique.

The other locking technique, *polarization spectroscopy* laser locking, uses the input signal of *polarization spectroscopy* and tries to find a diode laser output current corresponding to the resonant frequency of atoms, v_0, and set the current to the found value. In the *polarization spectroscopy* locking technique the diode laser scans through a range of frequencies with the help of a *LabVIEW* computer program. The program locates resonant frequency of the absorption of indium atoms in a hollow cathode (*HCL*) lamp by finding the maximum point or the inflection point of the input signal, and finds the corresponding diode laser current of the point, and then sets the diode laser frequency to the found frequency and periodically repeats this process to stabilize the laser to a transition.

The second part of the thesis uses the locking techniques for temperature measurements in a flame. A *two-line atomic fluorescence* (*TLAF*) thermometry technique is selected for temperature measurement studies. This technique uses seeded metallic

atoms (indium in this case) in a flame for temperature measurements. The temperature measurement is done by exciting electrons from two lower states of indium atoms to a common upper state and measuring the relative fluorescence signal of each transition. The fluorescence signals are proportional to the population in each lower state governed by the Boltzmann distribution which is dependent on the temperature of the system. The locking techniques explained in the first part of the thesis are used to stabilize a laser frequency to the transitions of indium. The indium atoms seeded into the flame are used to get a *2D* map of temperature in a laminar flame. The temperature information is crucial for understanding the flame interactions and reactions.

A) LASER LOCKING

In the first part of this thesis two different methods of locking a diode laser to a specific molecular transition will be discussed, i.e. *wavelength modulation spectroscopy* and *polarization spectroscopy*.

2. Tunable diode laser absorption spectroscopy

The simplest way to separate wavelengths of signal light of a gaseous sample is to use a monochromator. Another way of separating the wavelengths is to use a single frequency light source, such as laser. The laser wavelength can be a function of time. Recording the absorption intensity on a detector as a function of time allows a spectroscopy without the need of a monochromator and improves detection signal to noise ratio by allowing the use of large areas of detectors. These advantages have made the tunable diode laser spectroscopy an obvious choice for fast and sensitive gas measurements [2].

2.1 FUNDAMENTAL PRINCIPLES OF TUNABLE DIODE LASER ABSORPTION SPECTROSCOPY

A simple schema of *tunable diode laser absorption spectroscopy* (*TDLAS*) setup is shown in *Figure 1*; it consists of a tunable diode laser, a sample cell and a detector that records the intensity of the laser as a function of time. Directing the laser to a Fabry Perot Etalon while tuning the laser gives the possibility of converting the time scale to frequency.

Figure 1 A basic TDLAS setup. As the laser is tuned over an absorption line, the transmited intensity will be recorded as a function of time on the detector.

In *Figure 2* the intensity of the laser before and after passing through the gaseous cell is shown as a function of time. The absorption peak appears when the laser frequency is scanned across the resonant absorption frequency of the gaseous sample [3].

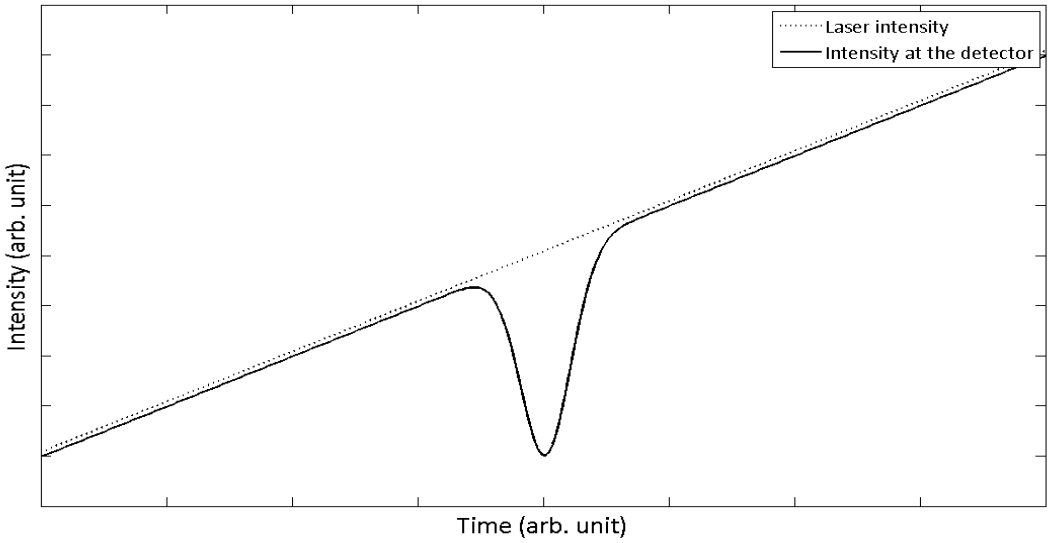

Figure 2 Intensity of light as a function of time, before (dotted line) and after (solid line) passing through the smaple cell.

The intensity of the absorbed light follows the Beer-Lambert law:

$$I(\omega) = I_0(\omega)\, exp(-\sigma(\omega)cL) \qquad (1)$$

where $I(\omega)$ is the intensity of the transmitted light at the frequency (ω); c is the concentration of the gaseous sample; L is the sample cell length, and σ is the frequency dependent absorption cross-section. The absorption cross-section, σ, is a sample molecule property and can be theoretically calculated or experimentally measured.

Although *TDLAS* technique, because of a simple setup, is commonly used in concentration measurement of gaseous samples, using *TDLAS* for measurements in samples with low concentration or gases with low absorption cross-section is not preferable [4], due it being sensitive to gas temperature, pressure, noise, laser power fluctuation, and varying background conditions [5].

Reducing background and noise would improve the sensitivity and increase the robustness of *TDLAS* technique for low concentration measurements. Modulation technique, such as wavelength modulation technique, is a common way of reducing the background [5].

2.2 WAVELENGTH MODULATION SPECTROSCOPY

The basic principle of *wavelength modulation spectroscopy* (*WMS*) is to sinusoidally modulate the laser frequency, with a modulation frequency ω_m, while still scanning the laser over the absorption line as in *TDLAS*. The signal detection in *WMS* is moved to higher frequencies to reduce signal to noise ratio as the noise often follows a $1/\nu$ relationship, where ν is the frequency. The *WMS* signal detection is done in multiples of the modulation frequency which is called harmonics or overtones.

In *WMS* the modulated signals are coherent in frequency and phase, in this sense any noise that does not contribute to the detection frequency centered around the modulated frequency will be also eliminated.

In a diode laser different frequencies are normally produced by a change in the input current of the laser, production of shorter frequencies needs higher current which increases the intensity. This effect is called *residual amplitude modulation* (*RAM*). Because of *RAM* effect, the intensity of the laser changes in absence of any sample.

The *RAM* effects are normally close to linear (because of direct relation between *RAM* and diode laser current) and their contribution to the higher order components of the absorption is tiny; in other words, in the absence of any sample the higher order components of diode laser output arising only from *RAM* and are close to zero. A major limiting factor of using the first harmonic (*1f*) detection in *WMS* technique is the large background arising from the *RAM* effect [6].

The higher harmonics arise due to nonlinearity of molecular absorption. Higher harmonics can be related back to the spectral absorption of the sample gas and used to infer the gas property.

The second harmonic (*2f*) signal parameters, such as linewidth, can be used for developing an algorithm to calculate absolute concentration of the sample species [7], the first harmonics signal (*1f*) also can be used for concentration and pressure measurements [3]. *Figure 3* shows the absorption peak with the first four harmonics generated by simulation.

The conventional way of implementing *WMS* is to modulate a diode laser with current produced as the summation of a slow linear sweep (sawtooth or triangle) scan function and sinusoidal modulation function. The resulting modulated electric field of the laser output is:

$$E(t) = E_0 \, exp[\, i(\, \omega_0 \, t \, + \, M \, sin(\omega_m \, t))] \qquad (2)$$

where ω_0 is the center frequency; M is the modulation index, and ω_m is the modulation frequency. The modulation index M is a key parameter in determining the exact form of

the signal and is defined as the ratio of the peak wavelength deviation around the center wavelength (scan amplitude) to the full width half maximum (*FWHM*) of the absorption line (Γ).

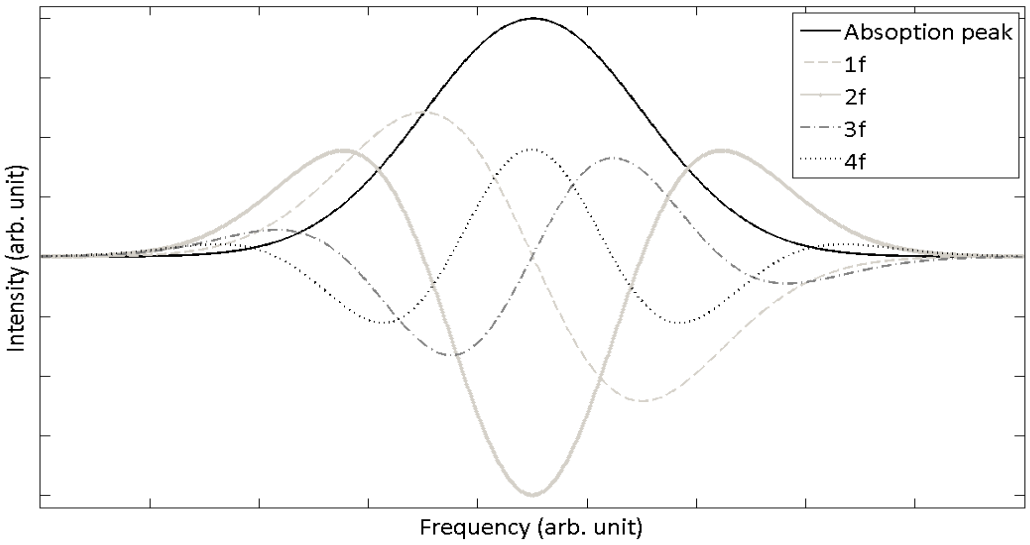

Figure 3 Simulated Gaussian absorption peak and its first four harmonics.

Experiments with different values of M and ω_m are described separately in literatures [8] [3] [6]. Because of instrumental difficulties, techniques with relatively low modulation frequencies were implemented at first.

Wavelength modulation (*WM*) spectroscopy is characterized by the use of low modulation frequency ω_m (much smaller than spectral *FWHM*, $\omega_m \ll \Gamma$) and high modulation index ($M \gg 1$).

In the case of frequency modulation (*FM*) spectroscopy, an external phase modulator is used to produce a pair of weak side-bands centered around carrier frequency. Frequency modulated wave has large modulation frequency, much greater than *FWHM* ($\omega_m \gg \Gamma$), and small modulation index, $M \leq 1$ [9].

For small M ($M < 0.2$) the n^{th} harmonic is proportional to the n^{th} derivative of the absorption profile, therefore for these values of M, the modulation technique may be called the derivative spectroscopy [10].

In recent years, analogue lock-in amplifier has been replaced by digitally recorded signals and the signal detection has been conducted in the post-processing. The technique is generally referred to as *digital wavelength modulation spectroscopy* (*dWMS*) [2].

2.2.1 dWMS analysis by Fourier methods

Higher harmonics may be detected by applying the Fourier transform to digitized signal. In Fourier transformed *dWMS* signal higher harmonics appear as sidebands around the modulation frequency. The *dWMS* input signal is detected in time domain, Fourier transform (*FT*) or fast Fourier transform (*FFT*) transforms the time-domain signal into the frequency-domain signal. *Figure 4 (a)* shows the modulated signal absorbed by *HCL* indium atoms in time domain. The x-axis conversion from time scale to frequency is done by a Fabry Perot etalon.

Figure 4 (b) shows fast Fourier transform of the input signal. Sidebands located on the both sides of the central frequencies are related to higher harmonics, a super-Gaussian window positioned over sidebands is used to separate harmonics, in *Figure 4 (b)* the super-Gaussian window is positioned over the second sideband.

In *dWMS* experiments absorption peaks are normally approximated by the Voigt profile, but in the limit of low pressure and high temperature or high pressure and low temperature the peaks can be approximated by a Gaussian or Lorentzian profile, respectively.

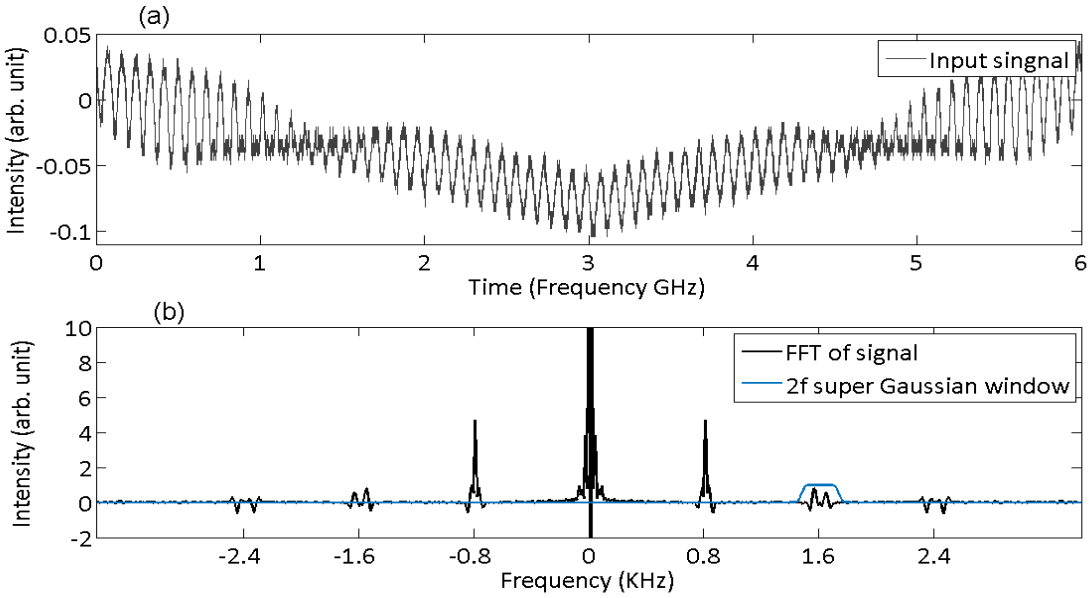

Figure 4 (a) dWMS input signal in time domain, (b) FFT of the input singal and a super-Gasussina window positioned over second harmonic.

2.2.2 Fourier component and absorption peak profile

As mentioned before, the transmitted laser intensity after passing a sample cell with the length of L is:

$$I(\nu) = I_0(\nu)\, exp(-\alpha L) \tag{3}$$

where α is a frequency dependent absorption coefficient.

For $\alpha \cdot L \leq 0.05$, *equation 3* may be written as:

$$I(\nu) = I_0(\nu)[1 - \alpha L] \tag{4}$$

The sinusoidally modulated diode laser output frequency in time domain is:

$$\nu_d(t) = \bar{\nu}_s + a_m\, cos(\omega_m t) \tag{5}$$

where $\bar{\nu}_s$ is the carrier frequency (scan frequency) of the diode laser and is slowly tuned by ramping the diode laser current in a sawtooth or triangular pattern; a_m is the modulation amplitude and ω_m is the modulation frequency of the diode laser. The

modulated output frequency of a diode laser is proportional to the input current, assuming that the intensity of the diode laser is independent of the input current, meaning no *RAM* effect, hence for small changes in the diode laser frequency:

$$I_0(\nu) \approx I_0(\nu_0) \approx I_0 \tag{6}$$

where v_0 is the resonant frequency of absorption peak. Therefore the time dependent term of intensity, $I(\nu(t))$, is an even function of time (because of the cosine function) and can be expressed as a cosine Fourier series:

$$I\big(\nu(t)\big) = \sum_{n=0}^{\infty} H_n(\bar{\nu})\, cos(n\, \omega_m t) \tag{7}$$

where $H_n(\bar{\nu})$ is the n^{th} Fourier component of Fourier series and can be selected using the super-Gaussian window [10].

For sufficiently small modulation amplitudes (derivative spectroscopy) the output signal components (harmonics) are proportional to the absorption line derivative and the Fourier components can be expressed as [10]:

$$H_n(\bar{\nu}) = \frac{2^{1-2}}{n!} a^n \frac{d^n \alpha(\nu)}{d\nu^n}\Big|_{\nu=\bar{\nu}}, \qquad n \geq 1 \tag{8}$$

The absorption peak profile for high pressures case is governed by collisional broadening and can be expressed by a Lorentzian function [10]:

$$\alpha^L(x, M) = \frac{1}{1 + [x + M\, cos(\omega t)]^2} \tag{9}$$

where two dimensionless parameters of x and M are defined as:

$$x = \frac{\bar{\nu} - \nu_0}{\Delta\nu}, \qquad M = \frac{a_m}{\Delta\nu} \tag{10}$$

In the case of low gas pressures and high temperature, the collisional broadening is negligible and the absorption line shape is Doppler broadened, described by a Gaussian profile [10]:

$$\alpha^G(x, M) = exp\left(-ln2\big(x + Mcos(\omega t)\big)^2\right) \tag{11}$$

The absorption profile of an intermediate case, where the collisional and Doppler broadening *FWHMs* are approximately equal, is called Voigt profile and is then a convolution of a Gaussian profile and a Lorenztian profile.

Figure 5 shows a second harmonic maximum positive value *P* and maximum negative value *N*. *R* is the ratio of *P* to *N*.

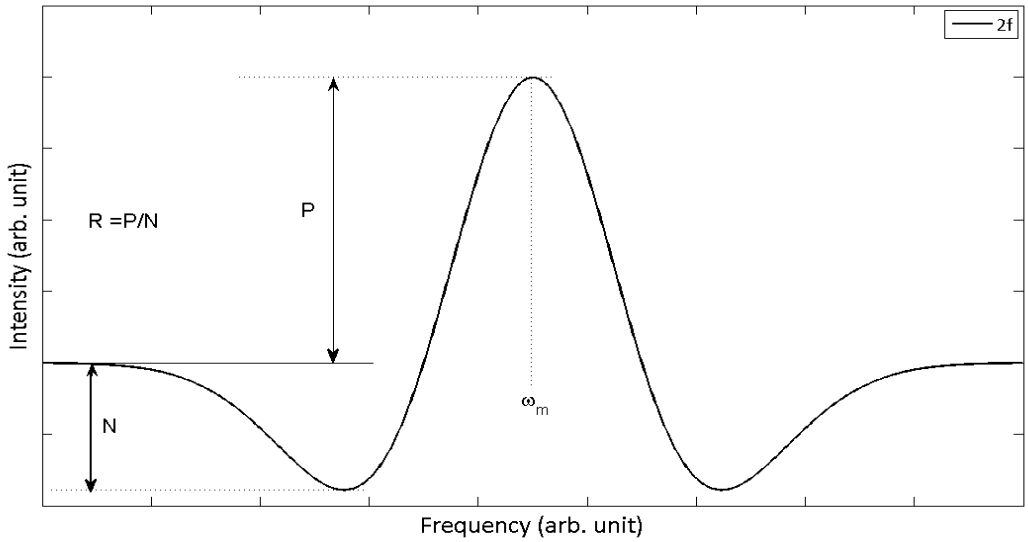

Figure 5 Maximum positive value, P and maximum negative value, N and the ratio of P to N, R (R = P/N) of a second harmonic.

Figure 6 shows a second harmonic's *P* and *R* parameters as a function of *M*. *Figure 6 (a)* shows the maximum positive value *P* of a second harmonic as a function of modulation index for Lorentzian, Gaussian, and Voigt profiles, the *P* value is maximized for *M* about *2.2*,

Figure 6 (b) shows *R*, the ratio of *P* to *N*, as a function of *M* for Gaussian, Lorentzian and Voigt line shapes. The *R* is a useful experimental parameter as it can be measured directly without the need for calibration and independent from the laser power. The *R* values of Gaussian, Lorentzian and Voigt profiles are converging for *M* about *2.2*.

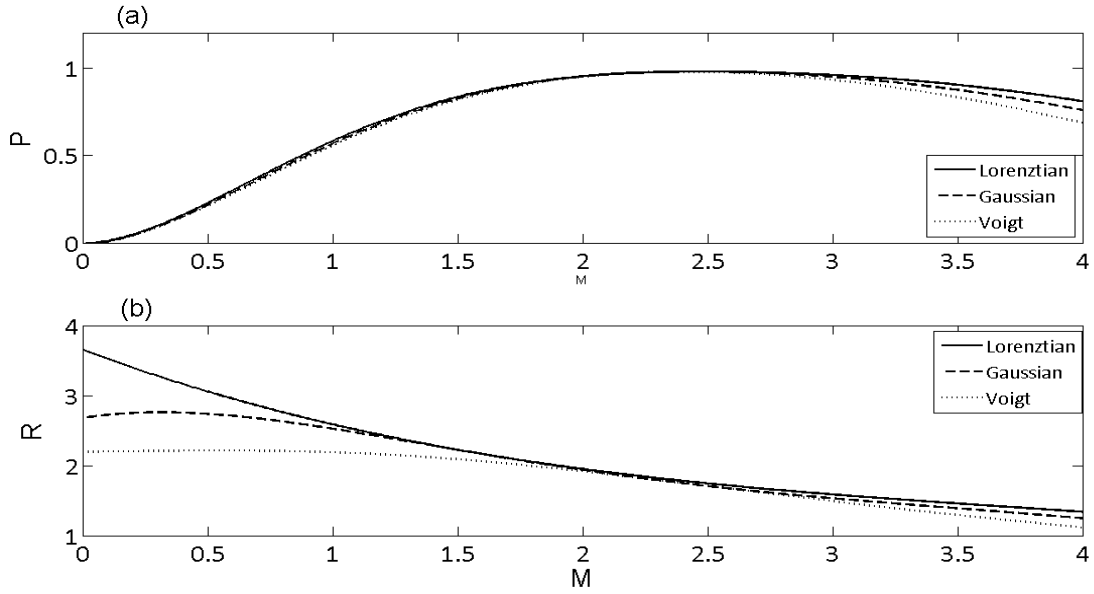

Figure 6 (a) P as a function of M for Gaussian, Lorentzian, and Voigt profile. Different profiles maximize and converge for M ≈ 2.2, (b) R as a function of M, different profiles converge for M ≈ 2.2, taken from [10].

2.3 DATA MEASUREMENT

The *wavelength modulation spectroscopy* is done by modulating the diode laser input current as:

$$I(t) = I_0 + a_s\, sawtoth(\omega_s) + a_m sin(\omega_m) \tag{12}$$

where I_0 is the current offset, a_s is the scan amplitude and ω_s is the scan frequency and a_m and ω_m are the modulation amplitude and frequency, respectively.

LabVIEW software is used to write a program for modulating output signal and demodulating and analyzing the *dWMS* signal. *Figure 7* shows the *LabVIEW* code layout.

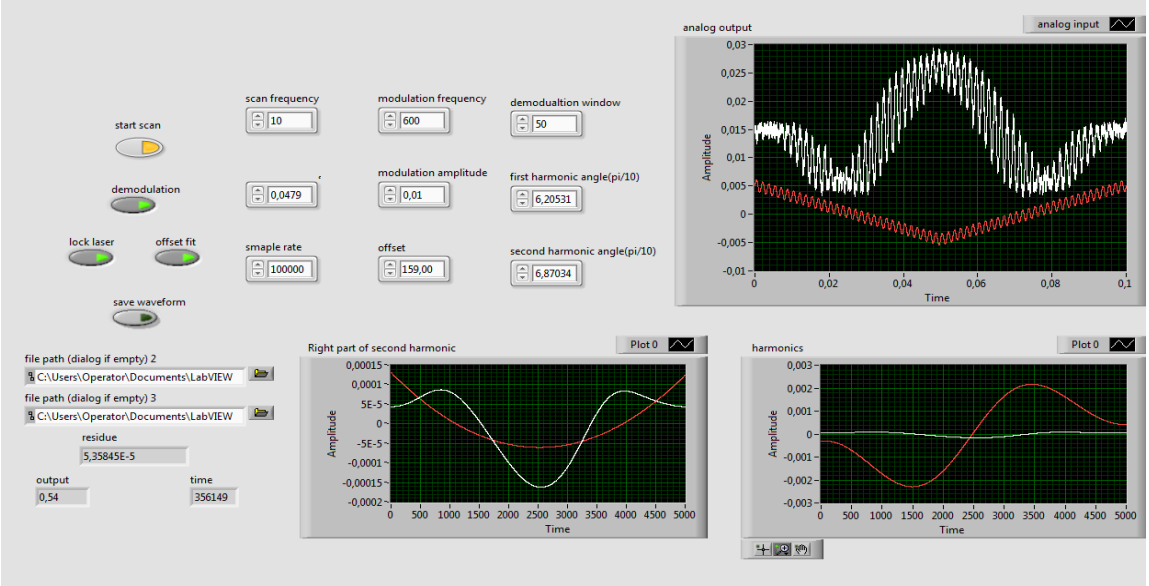

Figure 7 The dWMS program layout written in the LabVIEW software.

2.3.1 Setup

The *dWMS* frequency stabilization setup, shown in *Figure 8,* consists of an external cavity diode laser, a hollow cathode lamp, a photodiode detector, a data acquisition card, a computer, and optical elements. A *TOPTICA DL 100 pro design* tunable diode laser is used to sweep the diode laser frequency in *410 nm* range with the maximum power of *13 mW*. The *TOPTICA* diode laser uses an external cavity and a grating to produce very narrow linewidth light that can scan through a range of wavelengths. Technical information about the *TOPTICA* tunable diode lasers is available on *TOPTICA OPTICS* website [11].

The laser is controlled by a *TOPTICA DC 110 supply and control rack*. A *DCC 110* current control module, a *DTC 110* temperature control module, and a *SC 100 HV scan generator* are included in the *supply and control rack* [11]. The *DCC* and *DTC 110* modules are included to control the current and temperature, respectively.

The *SC 110 HV scan generators* is able to generates a triangle wave or send a computer generated signal to the diode laser.

A National Instrument data acquisition (*DAQ*) card, *NI USB-6363*, is used to communicate with the diode laser supply and control rack and the photodiode detector. The *DAQ* card converts the digital *LabVIEW* modulated signal into the analog output current and sends it to the diode laser rack and also converts the analog output current of a photodiode to the digital signal and imports it into the *LabVIEW* program. More information about the *DAQ* card is available on the *NI* website [12].

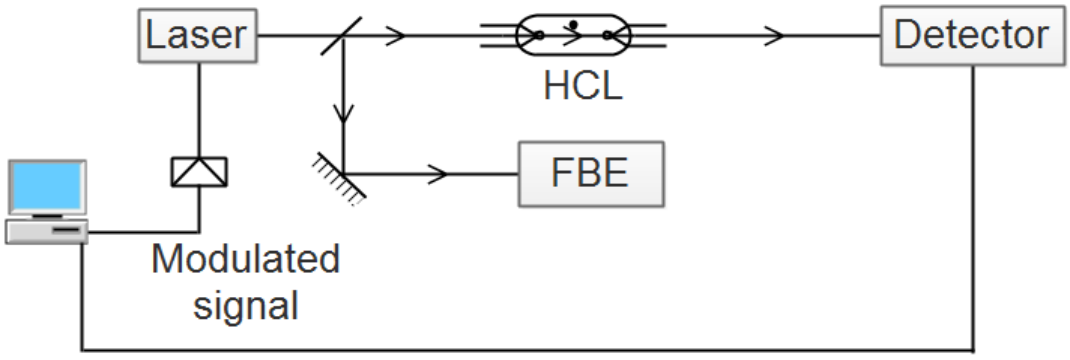

Figure 8 Schematic of digital signal modulation and demodulation, Fabry Perot ethalon is used for calibration of time domain to frequency domain.

A *Heraeus Noblelight 37 mm* hollow cathode lamp with the maximum current of *10 mA* is used as a source of indium atoms. In the *HCL* a large voltage across the anode and cathode excites and ionizes neon gas atoms and creates a plasma of neon gas inside the tube. Then the ionized neon atoms accelerate toward the cathode and sputter off indium atoms from the cathode that are probed with the laser. The *Heraeus Noblelight* website contains more technical information about the *HCL* lamp [13].

2.3.2 Frequency stabilization process

The *LabVIEW* program generates a modulated current with different scan and modulation parameters based on *equation 12* while the scan frequency and modulation frequency are kept constant ant *10 Hz* and *800 Hz*, respectively. The diode laser then converts the input modulated current into the frequency modulated laser signal. Then the modulated signal passes through the *HCL*. The photodiode records the transmitted laser intensity passed through the *HCL*. The *dWMS* locking software tries to stabilize the laser frequency around an indium transition by reducing the scanning range of the modulated current thus the diode laser output frequency range.

A demodulation program is used in the *dWMS* locking program to demodulate the input signal from photodiode using Fourier based demodulation technique. *Figure 9 (a)* shows the *dWMS* locking program generated signal with the scan frequency of *10 Hz*, modulation frequency of *800 Hz*, scan amplitude of *7.5979 GHz*, modulation amplitude of *949.7 MHz*, and the sample rate of *100000* samples per second. *Figure 9(b)* shows the photodiode output signal of *dWMS* corresponding to *410 nm* transition of indium atoms. *Figure 9 (c)* shows the Fourier transform of the *dWMS* signal, in which higher harmonics as sidebands are positioned around the central frequency. The demodulation program uses a super-Gaussian window positioned on different sidebands to separate different harmonics of the input signals.

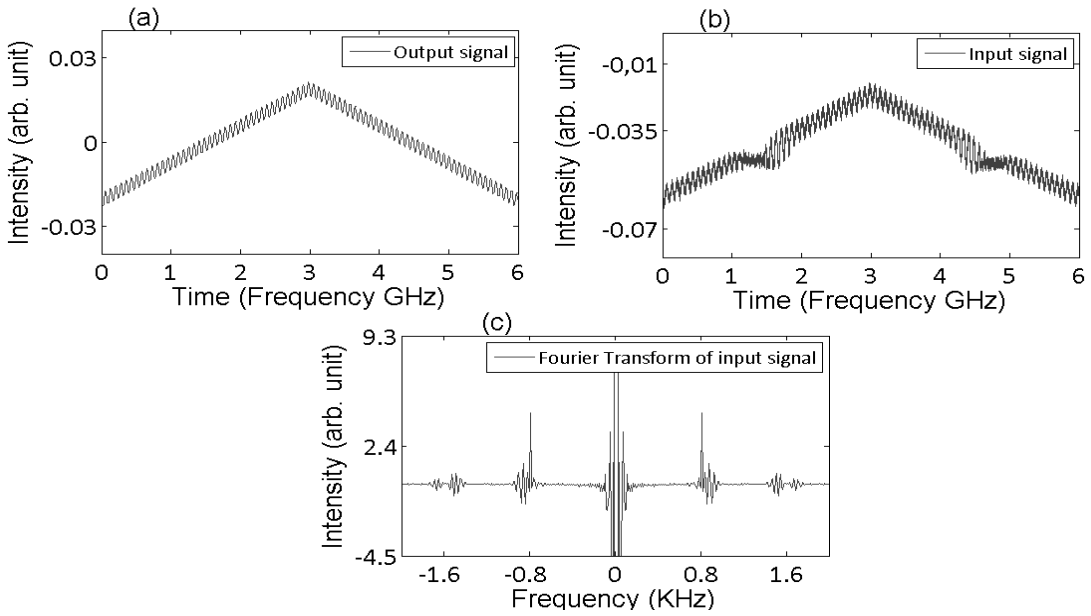

Figure 9 (a) The dWMS program output signal, (b) the dWMS input signal, (c) Fast Fourier transform of the input signal.

Figure 10 (a) shows the super-Gaussian functions positioned on fast Fourier transform (*FFT*) of the input signal, by positioning a super-Gaussian function over the first or second sideband, the first or second harmonic of the input signal (*Figure 10 (b)*) may be acquired. The result of multiplication of carefully positioned super-Gaussian windows with *FFT* of the input signal consists of different *FFT* sidebands, i.e. in *Figure 10 (a)* the *FFT* signal multiplied by the red colored super-Gaussian window separates the first sideband and the *FFT* signal multiplied by the blue colored super-Gaussian window separates the second sideband. *Figure 10 (b)* shows the first and second harmonics of the input signal. The reverse Fourier transform of the first and second sidebands generates the first and second harmonics of the input signal in time domain. These harmonics then have been used in locking process.

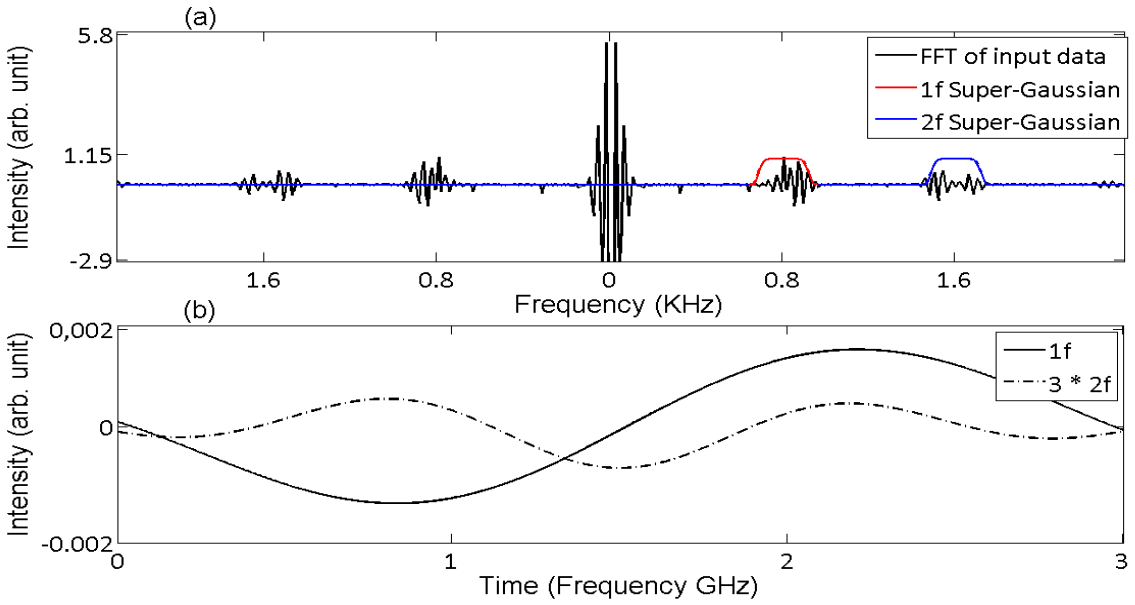

Figure 10 (a) Super-Gaussian windows positioned over the first and second sidebands of the FFT input signal, (b) The first and second harmonics of the dWMS signal.

The *dWMS* locking program keeps the indium atoms' absorption peak in the middle of the scanning range by maintaining the inflection point of first harmonics in the middle of the plot. To lock the laser to a specific transition of indium atoms, the program constantly reduces the scanning amplitude of the laser around the resonant frequency and simultaneously tries to fit a quadratic function into the second harmonic of the *dWMS* signal. During the second harmonics fitting, the program minimizes the fitting residual by reducing the scanning amplitude. The scanning amplitude reduction decreases the fitting residual to a point that scanning amplitude reduction deforms the second harmonic thus increases the fitting residual. The second harmonics deformation point caused by the scanning amplitude reduction is the limit of frequency stabilization by *dWMS* technique. Replacing the simple quadratic fitting function by a second derivative of a Gaussian function improves the diode laser frequency stabilization output.

In *Figure 11*, the *dWMS* input signals are shown on the left and the quadratic functions (red curves) fitting and second harmonics (blue curves) of the input signals are shown on the right. Continuous reduction of the scanning amplitude reduces the fitting residuals of quadratic functions to the second harmonics, as can be seen in *Figure 11*. Smaller scanning amplitude as it is shown in *Figure 11(d)* means shorter frequency interval and smaller fitting residual and more stabilized laser.

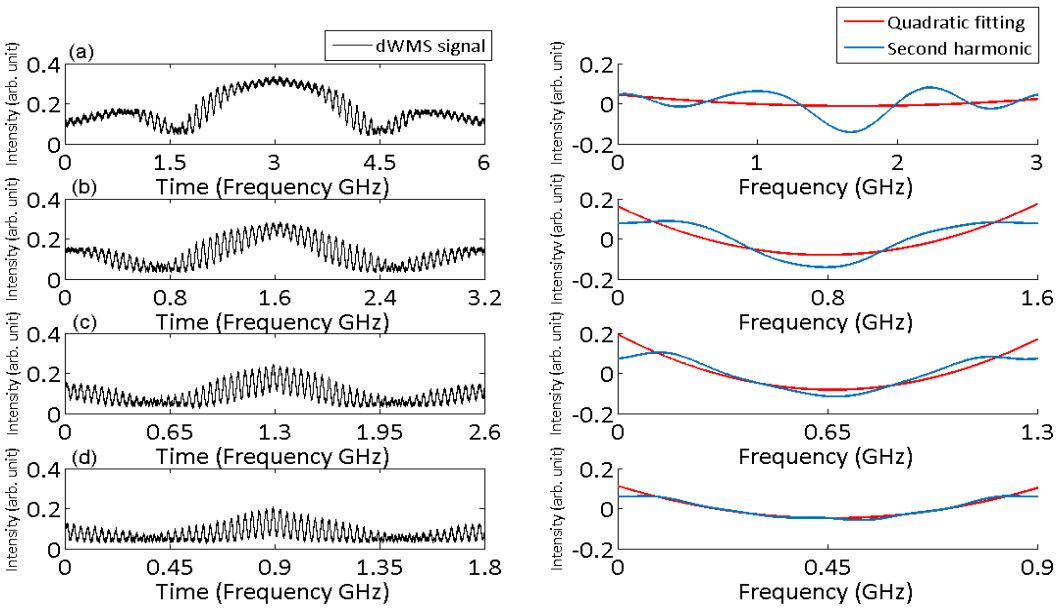

Figure 11 The dWMS input signals (right) and second harmonics and quadratic fitting functions (left) for scanning amplitudes of (a) 3.0866 GHz, (b) 1.6108 GHz, (c) 1.0295 GHz, and (d) 687.6 MHz.

Two different d*WMS* locking programs are tried for laser locking; the first program keeps the modulation amplitude constant during the locking process and only reduces the scanning amplitude, the second program reduces the scanning amplitude and modulation amplitude in the locking process. The diode laser frequency range is equal to sum of scanning and modulation amplitude and in the first algorithm is limited by the modulation amplitude. In the beginning of the program the scanning amplitude is much

bigger than the modulation amplitude and the effect of modulation amplitude on the frequency range is negligible, continuous reduction of the scanning amplitude leads to a point that the scanning amplitude is comparable to the modulation amplitude and the effect of modulation amplitude on the frequency range is significant.

The laser frequency minus the resonant frequency of a transition as a function of time is shown in *Figure 12*. The scanning amplitude reduction reduces the scanning frequency range around the resonant frequency of indium atoms to a point that lessening the scanning amplitude deforms the second harmonic and increases the fitting residual, shown in *Figure 12 (a)*, from this point on the program keeps the frequency range constant. *Figure 12 (b)* depicts the red rectangular area in *Figure 12 (a)* in more detail. The frequency interval of stabilized laser for this method is *712.86 MHz*, which is equal to a *400 fm* (4×10^{-13} *m)* wavelength interval; zero in plots are equal to *410.2871 nm* (data are the average of five measurements with the standard deviation of *35.53 fm).*

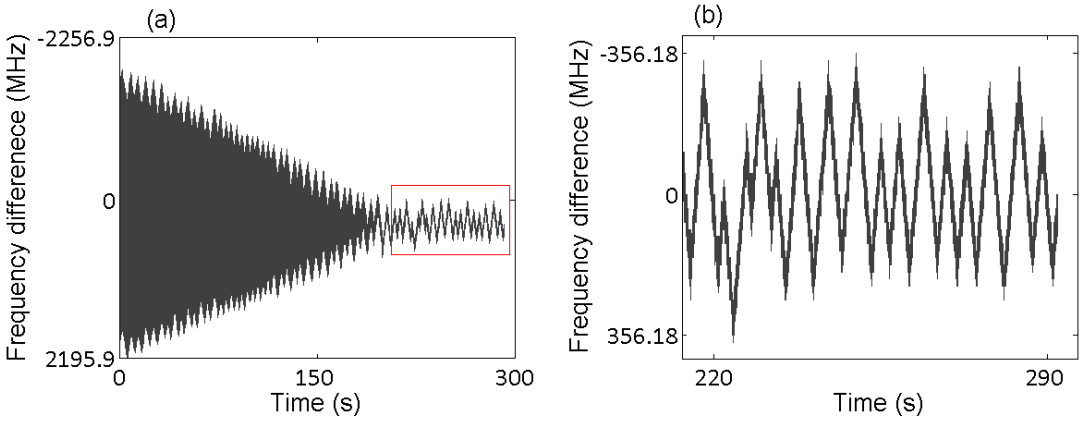

Figure 12 (a) The frequency output of the dWMS locking program to the 410 nm transition of indium atoms minus the resonant frequency as a function of time, while keeping the modulation amplitude constant, (b) a magnified view of the red box of (a).

The second algorithm decreases the modulation amplitude when it is greater than the scanning amplitude along with the reduction of the scanning amplitude to a point that reducing the scanning amplitude and modulation amplitude deform the second harmonic and increase the fitting residual; the result shows a better precision in diode laser frequency stabilization. *Figure 13* shows the diode laser frequency as a function of time for the second algorithm.

Figure 13 (b) shows that the stabilized laser frequency range of *249.50 MHz*, which is equal to the wavelength interval of *140 fm* (14×10^{-13} *m*) around the indium resonant wavelength of *410.2871 nm* (data are the average of five measurements with the standard deviation of (*41.83 fm*).

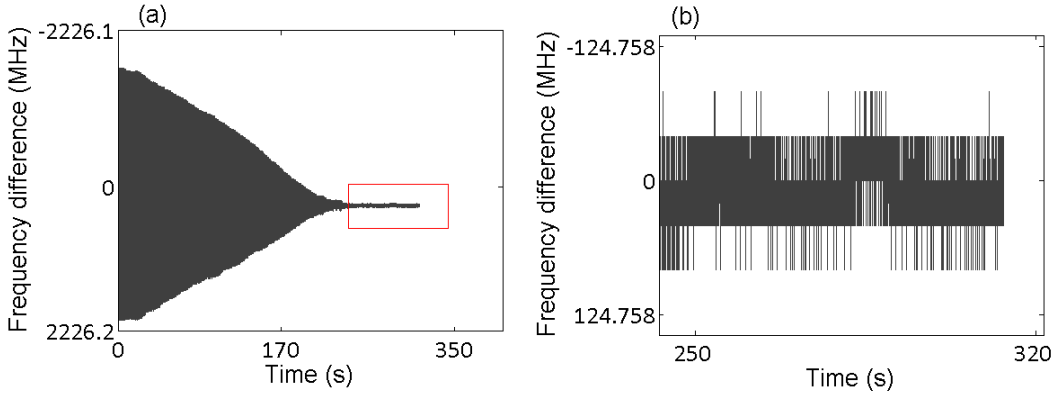

Figure 13 (a) The frequency output of the diode laser minus the resonant frequency of the transition as a function of time for the dWMS locking algorithm that reduces the modulation amplitude and the scanning amplitude simultaneously, (b) a magnified view of the red box of (a).

The second algorithm reduces the frequency interval by a factor of two compare to the first algorithm and produces more stable laser output.

3. Polarization Spectroscopy

Unlike *saturation spectroscopy*, which monitors the decrease of absorption of a probe beam caused by the depletion of some absorbing levels by the pump beam, the *polarization spectroscopy* (*PS*) signal is produced by the change in the polarization state of the probe beam induced by a polarized pump beam [14].

Optical pumping not only causes a change in the absorption coefficient, α, but also changes the refractive index, n, of sample molecules, resulting in a sensitive Doppler free technique with many advantages compared to normal saturation spectroscopy.

3.1 BASIC PRINCIPLE

The basic *PS* setup is shown in *Figure 14*. The laser output in this technique is divided into a probe beam with low intensity I_1, and a strong pump laser beam with the intensity I_2.

The probe beam passes through two linear polarizers, P_1 and P_2. These two linear polarizers are at a crossed position against each other, implying that in the absence of pump beam to change the polarization of the probe beam the detector does not receive any signal in the ideal situation, however, the detector will receive a small signal caused by a residual transmission of the crossed polarizers, normally smaller than $10^{-8} \times I_1$.

The schematic of *PS* setup is shown in *Figure 14*, the pump beam passes through a $\lambda/4$ wave plate changing the polarization of laser source form linearly polarized into a circularly polarized light.

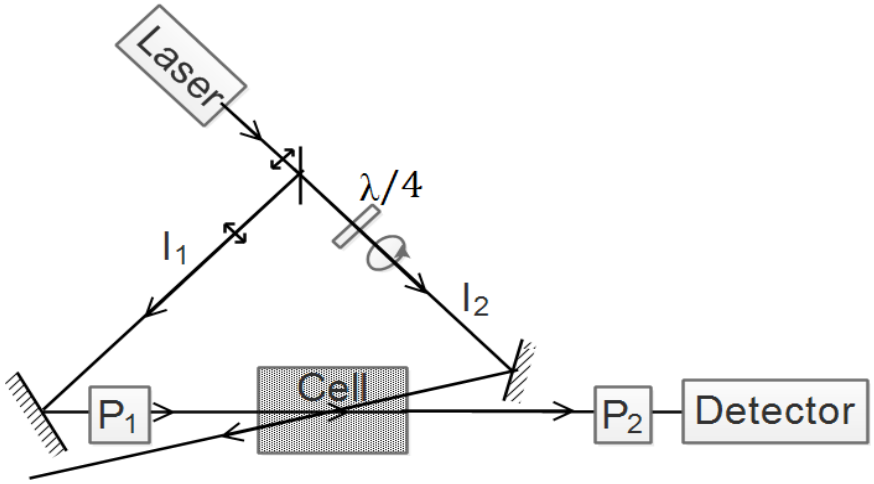

Figure 14 The schematic of polarization spectroscopy setup.

When the light frequency ω is tuned to the energy difference between the lower state (J'', M'') and the higher state (J', M') of a molecule, the (J'', M'') $\rightarrow$ (J', M') transition will take place. The quantum number M describes the projection of quantum number J into the Z-axis, arbitrary chosen in the laser propagation direction.

The selection rule for the transition of $M'' \rightarrow M'$ dictates that a change in the M quantum number should be one, $\Delta M = \pm 1$. In case of σ^+ circularly polarized light ΔM is limited to $+1$ and vice versa for σ^-. The pump light saturation causes some degenerate M'' sub-levels of the rotational level J'' to become totally or partially depleted. The depletion level of the M'' sub-levels depends on the intensity of the pump laser, absorption cross-section and the rate of relaxation that may repopulate the ground state. As can be seen in *Figure 15*, for P-transitions ($\Delta J = J' - J'' = -1$) and the selection rule of $\Delta M = +1$, some M'' sublevels (like $M'' = +J''$) are not pumped. For R-transitions ($\Delta J = +1$) some upper states like ($M' = -J'$) are not populated. These two processes will

lead to the production of unequal saturation and a non-uniform population of *M* sub-levels, meaning an anisotropic distribution of angular momentum *J* orientations.

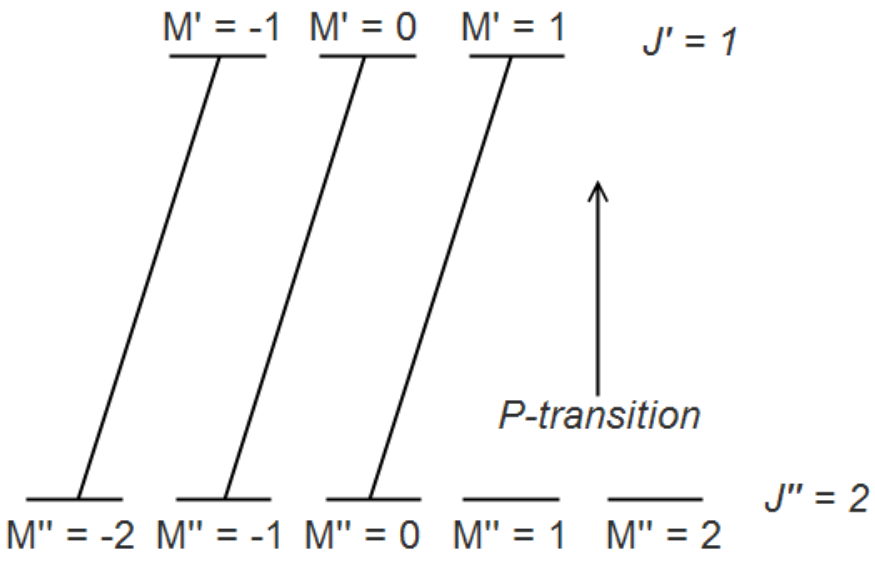

Figure 15 P-transition between a rotational ground state of J'' = 2 and rotational excited states of J' = 1.

The anisotropy caused by the non-uniform population produces a birefringent property in the sample. The birefringent property causes a slight rotation of a linearly polarized probe beam plane of polarization after passing through the anisotropic medium.

The anisotropic medium will be produced by the molecules with velocities of $v_z \pm \Delta v_z$, who are interacting with the strong pump beam, where:

$$v_z \pm \Delta v_z = (\omega_0 - \omega)/k \ \pm \gamma/k \tag{13}$$

where Δv_z is determined by the homogeneous linewidth, $\delta\omega = \gamma$.

When the laser frequency coincides with the resonant frequency ω_0, the pump and the probe beam affect the molecules in the same velocity group, so the probe beam will observe a birefringence effect, caused by the non-isotropic distribution of the molecules

that are produced by the pump beam. Here the plane of polarization of the probe beam will slightly rotate by an angle $\Delta\theta$, and the signal will pass through the second linear polarizer, P_2, so the detector will record a Doppler free signal.

3.1.1 Circularly polarized pump beam

A linearly polarized light can be written as a summation of two circularly polarized lights rotating in opposite directions, σ^- and σ^+. The electric field of a linearly polarized light can be written as summation electric fields of clockwise and counter-clockwise circularly polarized light ($E = E^+ + E^-$). When a light beam passes through a birefringent medium saturated by circularly polarized pump light, σ^+, the $\hat{x}$ and $\hat{y}$ components of the light experience different absorption coefficients of α^+ and α^-, also the light experiences different refractive indices n^+ and n^-. After passing the length L, in an isotropic medium the anisotropy causes a small phase shift and amplitude difference in the probe beam [14]:

$$\Delta\phi = (k^+ - k^-)L = \left(\frac{\omega L}{c}\right)\Delta n \tag{14}$$

$$\Delta E = \frac{E_0}{2}(exp-(\alpha^+/2)L - exp-(\alpha^-/2)L) \tag{15}$$

where $\Delta n = n^+ - n^-$, and $\Delta\alpha = \alpha^+ - \alpha^-$.

There is a small pressure induced birefringence effect caused by the difference between the atmospheric pressure outside the cell and the inside pressure, and also the absorption cell windows with the thickness of d affect the refractive index and the light absorption coefficient, these two effects are called window birefringence effect and are denoted by n_w and α_w, for the window refractive index and absorption coefficient, respectively.

In most of the experimental cases the difference in refractive index, Δn, and absorption coefficient, $\Delta\alpha$, are very small. By minimizing the cell windows birefringence the total electric field of the probe beam can be written as [14]:

$$E_t = E_0\, exp\, i\omega t\ \ exp\left(-i\left(\frac{\omega(nL + n_w)}{c} - \frac{i}{2}(\alpha L + a_w)\right)\right)(\theta\ + \delta) \tag{16}$$

Variable, δ is called the phase factor and depends on the difference of refractive index and absorption coefficient caused by the pump beam and cell window anisotropy. The detector signal, S(ω) is proportional to the transmitted intensity and can be written as:

$$S(\omega) \propto I_t(\omega) = c\epsilon_0 E_t E_t^* \tag{17}$$

Even in the $\theta = 0°$ case the cross polarizers have a small residual transition ($I_t = \xi I_0$), the transmitted intensity can be written as is [14]:

$$\begin{aligned} I_t &= I_0\, exp(-\alpha L - \alpha_w)(\xi + |\theta + \Delta|^2) \\ &= I_0\, exp(-\alpha L - a_w)\left(\xi + \theta'^2 + \left(\frac{1}{2}\Delta a_w\right)^2 + \frac{1}{4}\Delta a_w L\Delta\alpha + \frac{\omega}{c}L\,\Delta n + \left(\frac{\omega}{2c}L\Delta n\right)^2 + \left(\frac{L\Delta\alpha}{4}\right)^2\right) \end{aligned} \tag{18}$$

where $\theta' = \theta + (\omega/2c)\,\Delta nw$.

Only molecules with the velocities within the range of, $\Delta v_z = 0 \pm \gamma_s/k$, that are interacting with the pump and probe beam simultaneously contributing to the change in absorption coefficient.

The absorption coefficient, $\alpha(\omega)$, and the refractive index, $n(\omega)$, are related by the Kramers-Kronig dispersion relation [15], therefore, $\Delta n(\omega)$ may be written as:

$$\Delta n(\omega) = \frac{c}{\omega_0}\frac{\Delta\alpha_0 x}{1 + x^2} \tag{19}$$

By replacing *equations 19* into *equation 18*, the transmitted intensity of probe beam with circularly polarized pump beam can be written as [14]:

$$S^{cp} = I_t(\omega) = I_0\, exp\left(-\alpha L - a_w\left(\xi + \theta'^2 + \frac{1}{4}\Delta a_w^2 + \right.\right. \tag{20}$$

$$\left.\left.\frac{1}{2}\theta'\Delta\alpha_0 L\frac{x}{1+x^2} + \left(\frac{1}{4}\Delta\alpha_0\Delta a_w L + \left(\frac{\Delta\alpha_0 L}{4}\right)^2\right)\frac{1}{1+x^2} + \frac{3}{4}\left(\frac{\Delta\alpha_0 x}{1+x^2}\right)^2\right)\right)$$

3.1.2 Linearly polarized pump beam

Instead of circularly polarized pump beam, *PS* may be performed using a linearly polarized pump beam; the schematic of the linear polarization spectroscopy setup is shown in *Figure 16*, two linear polarized laser beams are used as pump and probe beam. The polarization difference between two beams is denoted by β and may vary between $\pi/2$ to $0°$ [16] [14].

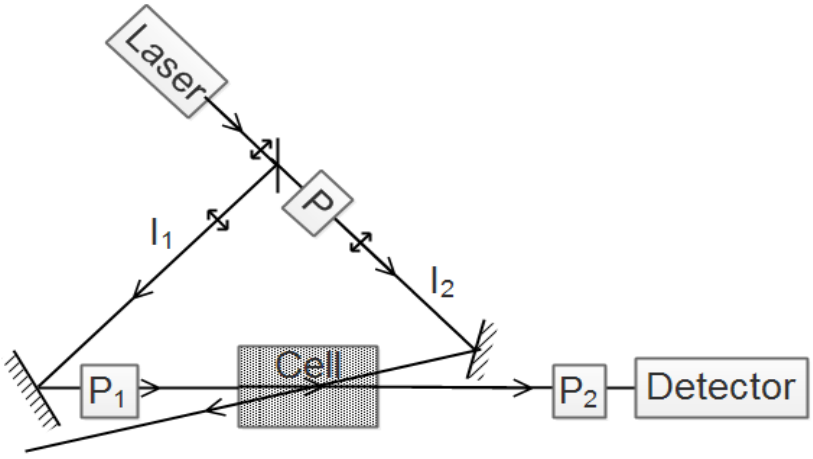

Figure 16 The polarization spectroscopy setup with the linearly polarized pump beam, the angle between pump and probe beam is generally 90°.

The linearly polarized probe beam can be decomposed into two different components, parallel and perpendicular to the pump beam. The pump beam induces different saturations for each of these components so the components will experience different absorption coefficients, $\Delta\alpha_{||}$ and $\Delta\alpha_{\perp}$. This anisotropy rotates the probe beam plane of polarization. The intensity of the probe beam passing through the anisotropic medium for $\beta = 45°$ can be rewritten as [16] [14]:

$$S^{LP} = I_t(\omega) = I_0\, exp\left(-\alpha L - a_w\left(\xi + \frac{1}{4}\theta^2\Delta a_w^2 + \left(\frac{\omega}{2c}\,\Delta b_r\right)^2 + \frac{\Delta b_r}{4}\frac{\omega}{c}\,\Delta\alpha_0 L\frac{x}{1+x^2} + \left(-\frac{1}{4}\theta\Delta\alpha_0\Delta a_w L + \left(\frac{\Delta\alpha_0 L}{4}\right)^2\right)\frac{1}{1+x^2}\right)\right) \quad (21)$$

where $\Delta\alpha = \alpha_{||} - \alpha_{\perp}$, and $b_r = b_{||} - b_{\perp}$, the angle θ is the angle between P_1 and P_2 polarizer. I_0 shows the detected intensity for $\theta = 0°$ and $\beta = 90°$, and in the absence of pump beam. L shows the length of the anisotropic medium inside the absorption cell [17].

3.2 DATA MEASUREMENT

LabVIEW software is used to write a program for data acquisition, signal generation and data analysis of an input signal. *Figure 17* shows the *LabVIEW* code layout.

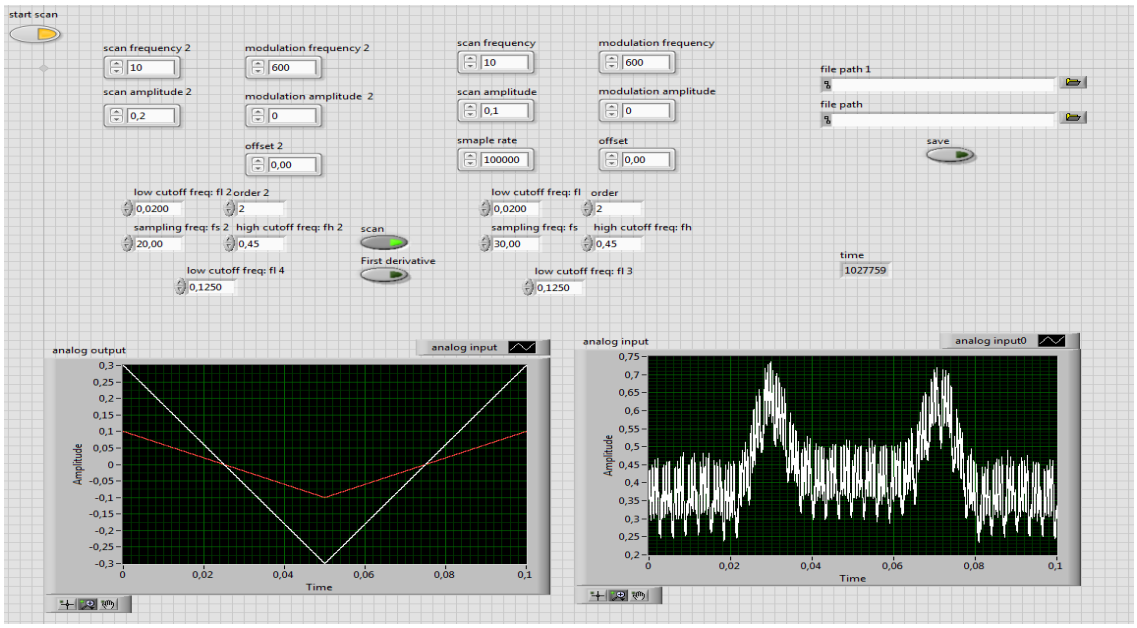

Figure 17 The LabVIEW's Polarization software layout.

3.2.1 Setup

A schematic of *PS* setup is shown in *Figure 18*, the *DAQ* card, supply and control rack, external cavity diode laser, photodiode detector, and the *HCL* are identical to *dWMS* setup.

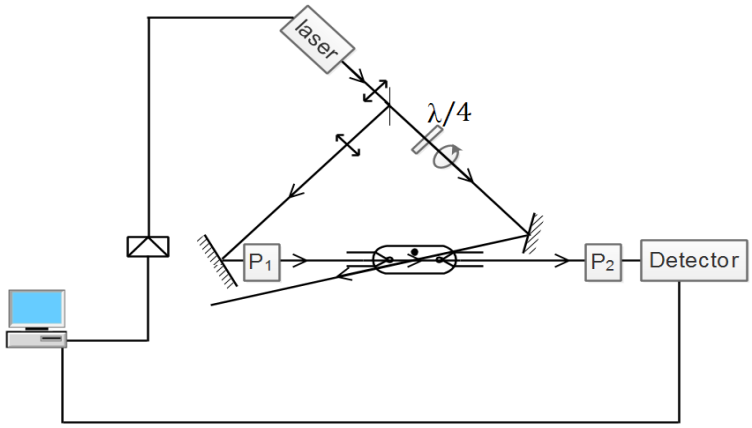

Figure 18 The schematic of polarization spectroscopy setup.

The only difference between a *dWMS* setup and a *PS* setup is in different optical elements. In a *PS* setup, a splitter divides the laser beam into a strong pump beam and a weak probe laser beam, the probe beam directly passes through two crossed polarizers, P_1 and P_2, and a hollow cathode lamp (*HCL*) and the intensity of the probe beam in the end will be recorded in a photodiode detector, the pump beam in normal *PS*, first passes through a quarter-wave plate to convert the linearly polarized light of a diode laser into the circularly polarized light, using adjustable mirrors, then the pump beam is directed to propagate in a direction opposite to the probe beam so that the two beams cross inside the *HCL* in an acute angle.

3.2.2 Frequency stabilization process

A polarization locking program is used to produce continuous sawtooth signal; a diode laser converts the generated signal into a sweeping laser signal covering a specific frequency range. A program written in *LabVIEW* inside the polarization locking software analyses the signal and locks the laser into indium atoms' transition .

The shape of recorded signal in the photodiode detector depends on the angle between two polarizers. For the angle $\theta = 0°$ and the scanning amplitude of *3.799 GHz* the signal shape is shown in *Figure 19 (a)*.

By slightly tilting the polarization angle from the crossed position, the signal will change to *Figure 19 (b)*.

The two input signals are used for locking a diode laser to a specific indium transition. The polarization locking program filters the *PS* input signals, shown by blue line in *Figure 19*, and finds the corresponding output current for the maximum of the filtered signal for $\theta = 0°$ case, (*Figure 19 (a)*), or the output current corresponds to the

inflection point of the filtered signal for the tilted case, (*Figure 19 (b)*), and set the diode laser output current to those values.

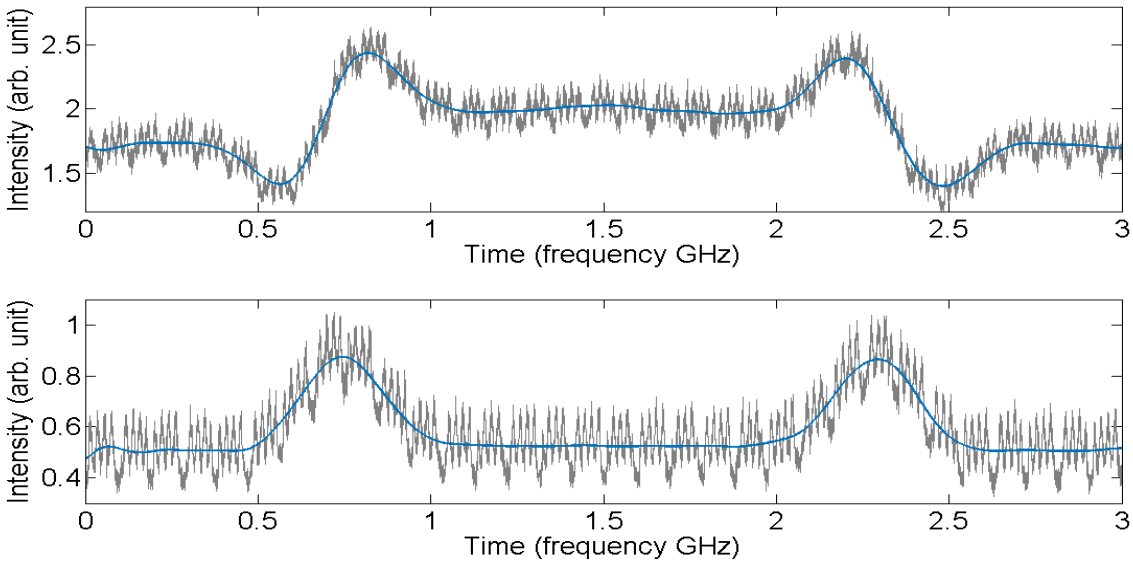

Figure 19 PS input signals and filtered signals for angle between two polarizers of (a) $\theta = 0°$, (b) $\theta = \epsilon°$.

The *PS* locking software consists of a loop with two time periods. First, for the scan period of *5000 ms* the software scans the laser in a specific frequency interval, filters the input signal, and finds the corresponding output current to the transition peak. Second, the locking period which starts form *5000 ms* and continues to *30000 ms*, during which the laser current is set to the current corresponding to the transition frequency of indium atoms. *Figure 20* shows the laser frequency output of the *PS* locking software, in this figure the scanning periods and the locking periods are recognizable, parts with the higher frequency interval are related to the scanning time, in the locking periods frequency changes are minimized and laser are stably fixed to the indium atoms' transition .

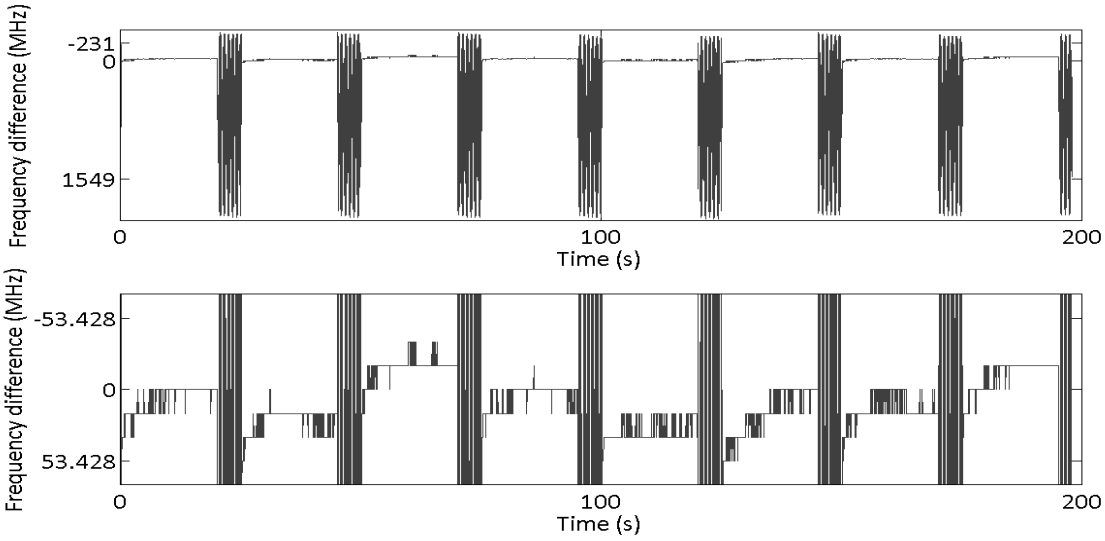

Figure 20 (a) The frequency output of the PS locking program minus the resonant frequency for the scan and locking periods, (b) zoomed on to the locking part of (a).

The wavelength changes in the scan periods depend on the scanning amplitude of the laser, for *Figure 20* the wavelength scanning interval is *1.4 pm* (1.4×10^{-12} *m*), which is equal to *2.4416 GHz* in frequency domain. The frequency interval for the locking part is *106.57 MHz*, which is equal to the wavelength interval of *60 fm* (6×10^{-14} *m*) around the transition wavelength of *410.2871 nm*. The data are the average of eight measurements, four measurements with $\theta = 0°$ and four measurements with slightly tilted θ, with the standard deviation of *7.56 fm* (7.56×10^{-15} *m*).

B) THERMOMETRY

The laser stabilization techniques developed in the first part of the thesis are being used in the second part to lock diode lasers to the *410 nm* and *451 nm* transitions of indium atoms for temperature measurements by *two-line atomic fluorescence thermometry* technique.

4. Two-line atomic fluorescence thermometry

4.1 LASER INDUCED FLUORESCENCE

Laser induced fluorescence (*LIF*) is a spectroscopic technique that has been used to study molecular structures, detection of species and to conduct temperature measurements in combustion process [1].

Fluorescence is the spontaneous emission of radiation from an excited state. In *LIF* molecules will be excited by a laser with a selected wavelength. The excited molecules then relax to the ground state by emitting light after a few nanoseconds. The emitted light will be recorded by the detectors such as photodiodes or cameras or be spectrally resolved with a spectrometer. The intensity of the emitted light is proportional to the density of the molecules in the ground state before excitation.

Figure 21 shows the energy diagrams of *LIF*, the bold horizontal lines show the vibrational states and narrow lines are depicting the rotational states. Fluorescence is a two-step process, absorption of light to excite the lower state, followed by emission of light from the excited state when it transitions back to a lower state. *Figure 21* shows the two types of *LIF* techniques that can be used to identify a species, in the fluorescence

spectrum (left), the laser is tuned to the specific absorption and the various emission transitions from the excited state to lower states will be recorded by spectrally dispersing the signal in a spectrometer. In the excitation scan (right), the laser is tuned to various absorption lines and the broadband total emission is recorded by the detector. Each of these two techniques will yield a unique spectrum depending on the probed molecule.

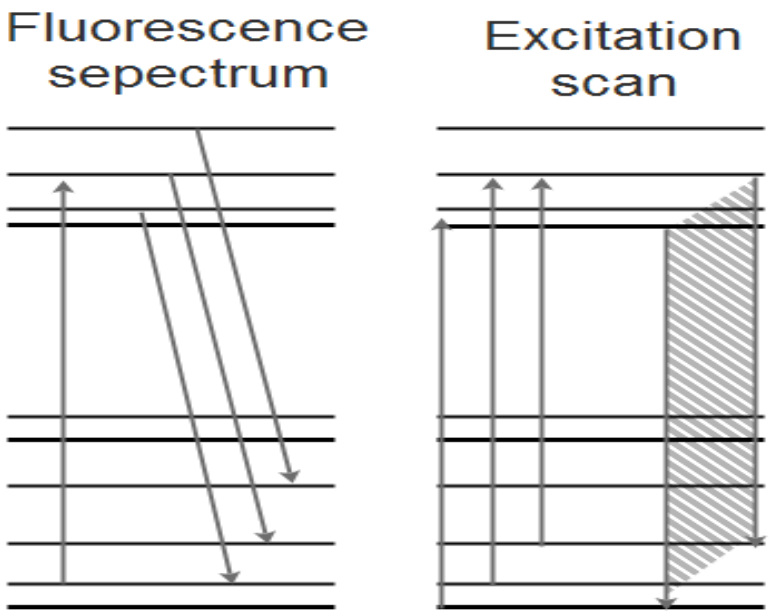

Figure 21 (left) Energy diagram of laser induced fluorescence, A laser is tuned to specific absorption and the fluorescence will be recorded excitation scan, (right) the laser is tuned to various absorption lines and total emission will be recorded.

4.1.1 Basic physics

A simple two-level system is shown in *Figure 22*. The rate constants for absorption, b_{12}, and stimulated emission, b_{21} are related to the Einstein coefficient of absorption and stimulated emission by:

$$b = \frac{BI_\nu}{c} \tag{22}$$

where B is the Einstein coefficient and I_ν is the incident laser irradiance per unit frequency ($^{W}/cm^2\ sec^{-1}$) [1].

Figure 22 shows the energy levels of a simple two-level system, A is the Einstein spontaneous emission rate constant, P is the pre-dissociation rate constant, W_{2i} is the photoionization rate constant and Q represents the collisional quenching rate constant.

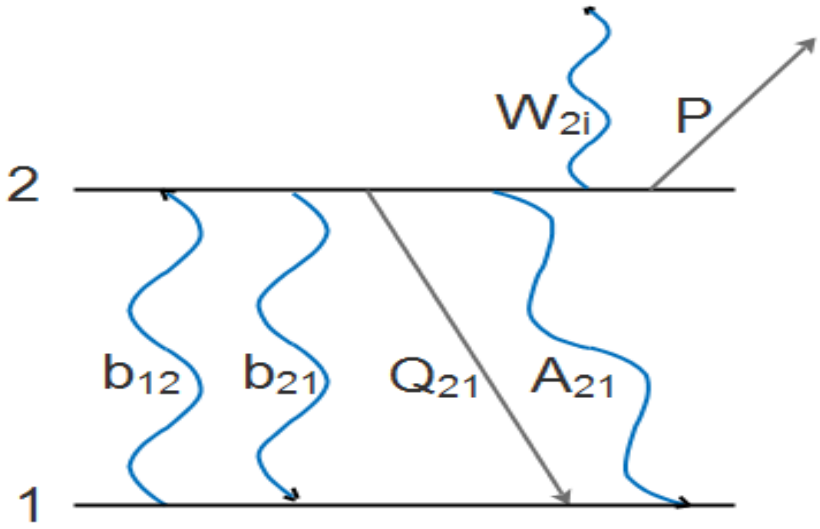

Figure 22 Different transitions in a two-level system, b_{12} and b_{21} are Einstein absorption coefficient and Einstein stimulated emission coefficient, respectively, A_{21} is Einstein spontaneous emission coefficient, Q_{21} is collisional quenching coefficient, P is pre-dissociation coefficient, and W_{2i} is photoionization coefficient.

The rate equation for the state of |1⟩ and |2⟩ is:

$$\frac{dN_1}{dt} = -N_1 b_{12} + N_2(b_{21} + A_{21} + Q_{21}) \tag{23}$$

$$\frac{dN_2}{dt} = N_1 b_{12} - N_2(b_{21} + A_{21} + Q_{21} + P + W_{2i}) \tag{24}$$

If photoionization and pre-dissociation are negligible, number of atoms in the |1⟩ and |2⟩ states stays constant.

The fluorescence signal is proportional to the spontaneous emission from state $|2\rangle$ to state $|1\rangle$, which depends on the number of atoms in the excited state and the spontaneous emission constant, (N_2A_{21}). The fluorescence signal power, F is [1]:

$$F = h\nu N_2 A_{21} \frac{\Omega}{4\pi} \ell A = h\nu \frac{\Omega}{4\pi} \ell A \, N_1^0 \frac{B_{12}}{B_{12} + B_{21}} \frac{A_{21}}{1 + \frac{I_{sat}^{\nu}}{I_{\nu}}} \tag{25}$$

where ν is the frequency of the emitted fluorescence; Ω is the collection solid angle; A is the focal area of the laser beam and ℓ is the axial extend along the beam from the observer point of view.

4.2 THERMOMETRY

Temperature measurements in a flame can be done by different methods. Rotational and Vibrational *coherent anti-Stokes Raman scattering* (*CARS*) is an effective technique for point measurements [18]. Thus *CARS* methods are accurate way of point temperature measurement in a flame. These methods are not used for two-dimensional thermometry. The filtered Rayleigh scattering method is a novel approach of two-dimensional thermometry [19]. *LIF* thermometry based on the naturally occurring species in a flame or on seeded atoms is another *2D* thermometry technique.

In *LIF* techniques the temperature measurement can be done by measuring the population distribution between two or more states [20]. Temperature measurement of molecular radicals is only done at high temperatures, needed to produce enough radials to reach an acceptable signal to noise ratio. For example, in *LIF* thermometry of *OH* radicals, the temperature should exceed the $1500° K$ [1]. The disadvantages of the molecular radicals *LIF* thermometry can be partially overcome by seeding the system with suitable atoms.

A *LIF* signal as described in *equation 25* depends on the collisional quenching *Q*, which for most realistic systems is unknown. Measuring the collisional information is difficult and in a turbulent system is not feasibly possible.

Two-line atomic fluorescence (*TLAF*) is an attractive fluorescence technique for measuring temperature. In *TLAF* technique the measurement is not affected by collisions.

4.2.1 Two-line atomic fluorescence thermometry

A simplified schematic of energy levels involved in *two-line atomic fluorescence* is shown in *Figure 23 (a)*. *TLAF* thermometry involves measuring the Stokes and anti-Stokes fluorescence signals. As shown *Figure 23 (a)*, laser light λ_{13} is used to excite the population from level $|1\rangle$ to level $|3\rangle$, then the Stokes fluorescence from level $|3\rangle$ to level $|2\rangle$, F_{32} is measured. After measuring the Stokes fluorescence signal, F_{32}, the laser light λ_{23} excites electrons from level $|2\rangle$ to level $|3\rangle$ and the anti-Stokes fluorescence, F_{31}, from the excited state to level $|1\rangle$ is measured. For turbulent flames both excitations can be performed in a short period of time, hundreds of nanoseconds, allowing the possibility to temporally resolve the temperature. The important feature of this technique is that the fluorescence signals, F_{31} and F_{32}, come from the same upper level, therefore the quenching factor for both fluorescence transitions are approximately the same. The relative intensity between the two fluorescence signals is dependent on the Boltzmann distribution, therefore the fluorescence intensities give information about the temperature.

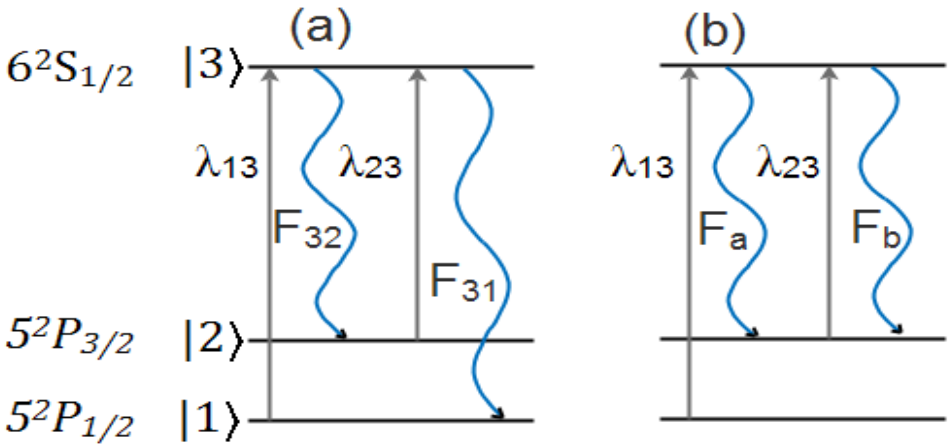

Figure 23 Energy diagram of the concerned energy levels in indium for (a) conventional TLAF,(b) modified TLAF.

The Stokes fluorescence from level |3⟩, pumped from level |1⟩ to level |3⟩ can be written as:

$$F_{32} \propto N_3 A_{32} = \frac{N_1 b_{13} A_{32}}{b_{31} + A + Q} \tag{26}$$

where $A = A_{31} + A_{32}$ and $Q = Q_{31} + Q_{32}$. The anti-Stokes fluorescence level |3⟩, pumped from level |2⟩ from level |3⟩ is:

$$F_{31} \propto N_3 A_{31} = \frac{N_2 b_{23} A_{31}}{b_{32} + A + Q} \tag{27}$$

The fluorescence signal ratio for the linear pumping case where $b << A + Q$ can be written as:

$$\frac{F_{31}}{F_{32}} = \frac{I_{23}\lambda_{32}^3}{I_{13}\lambda_{31}^3} exp\left(\frac{-(E_2 - E_1)}{kT}\right) \tag{28}$$

where E_1 and E_2 are the energies of levels |1⟩ and |2⟩, respectively [21] [1] [22].

4.2.2 TLAF thermometry of indium atoms

In *TLAF* thermometry of indium atoms, the indium atoms are seeded into the flame. Temperature can be measured by comparing the Stokes, *451 nm,* and anti-Stokes, *410 nm,* fluorescence signals, after excitation. The *TLAF* thermometry has been chosen because of its advantages over *LIF* thermometry. The first advantage is due to a common upper state which entails that the collision quenching is not affecting the temperature measurement. Furthermore, indium atoms have much higher transition strength compared to the molecular species, yielding a better signal to noise ratio. Spin-orbit splitting in *5P* ground state of indium atom leads to the energy splitting that ideally matches combustion temperatures, ranging from *1000-4000° K* [22].

The three $|1\rangle$, $|2\rangle$ and $|3\rangle$ levels of indium atoms are shown in *Figure 23 (a)*, these levels are the $5^2P_{1/2}$, $5^2P_{3/2}$, and $6^2S_{1/2}$ energy levels of indium atom respectively. Initially the $|1\rangle \rightarrow |3\rangle$ transition is pumped by λ_{13} and by using a proper filter the Stokes fluorescence F_{32} is detected. Then the $|2\rangle \rightarrow |3\rangle$ transition is pumped by λ_{23} and the anti-Stokes, F_{31}, fluorescence is detected using second filter.

Temperate T can be derived by rewriting *equation 28* as:

$$T = \frac{\Delta E/k}{ln\left(\frac{F_{32}/I_{13}^{v}}{F_{31}/I_{23}^{v}}\right) + 4\,ln\left(\frac{\lambda_{32}}{\lambda_{31}}\right) + ln\,C_1} \tag{29}$$

where I^{v}_{23} is the laser irradiance for λ_{23}, and I^{v}_{13} is the laser irradiance for, λ_{13}; ΔE is the energy separation between the two lower levels. The dimensionless calibration constant C_1 can be determined experimentally and accounts for the difference in the efficiency of detector for different wavelengths, the characteristics of different filters and the spectral overlap between the laser profiles and the atomic transitions. The relative detection efficiencies in the calibration are generally the main source of systematic errors.

Figure 23 (b) shows a different detection method for *TLAF* temperature measurements. In this method λ_{13} is used to pump the transition $|1\rangle \rightarrow |3\rangle$ and the Stokes fluorescence, F_a, is detected. The wavelength λ_{23} is used to pump the $|2\rangle \rightarrow |3\rangle$ transition and instead of detecting the anti-Stokes transition, F_{31}, as in conventional *TLAF* the resonance fluorescence, F_b is detected.

In modified *TLAF* only one wavelength will be detected, therefore only one band pass filter for *451 nm*, and one detector is needed and the sensitivity of detector for both fluorescence transitions is the same.

There are several reasons why modified *TLAF* technique is preferable; first, the oscillation strength of the fluorescence transition from level $|3\rangle \rightarrow |2\rangle$ at, *451 nm*, is almost two times stronger than the $|3\rangle \rightarrow |1\rangle$ transition at *410 nm*. As it is shown in *equation 26* and *equation 27* the fluorescence signals depend on the Einstein spontaneous emission constant and A_{32} is almost twice as big as A_{31} for indium atoms ($A_{32} = 1.02 \times 10^8\ s^{-1}$, $A_{31} = 0.56 \times 10^8\ s^{-1}$). Secondly, the flame emission at *451 nm* is lower compared to *410 nm*; thirdly, due to lower population of state $|2\rangle$ compared to state $|1\rangle$, less signal trapping happens in the *451 nm* at λ_{23} transition. The signal trapping is caused by re-absorption of the produced fluorescence signals by atoms in lower states.

The temperature of a modified *TLAF* technique can be written as:

$$T = \frac{\Delta E/k}{ln\left(\frac{F_a/I_{13}^{\nu}}{F_b/I_{23}^{\nu}}\right) + 3\,ln\left(\frac{\lambda_{32}}{\lambda_{31}}\right) + ln\left(\frac{A_{32}}{A_{31}}\right) + ln\,C_2} \tag{30}$$

The disadvantages in the modified techniques are the appearance of Einstein coefficient in the denominator of the equation and these coefficients need to be known. C_2 is the calibration constant need to be measured experimentally and includes the laser power corrections for λ_{13} and λ_{23}.

4.3 TEMPERATURE MEASUREMENT

A *LabVIEW* program, as previously described, is used to stabilize two frequencies of two diode lasers to $|1\rangle \rightarrow |3\rangle$ and $|2\rangle \rightarrow |3\rangle$ transitions of indium, at *410 nm* and *451 nm*, respectively. The locking program may use *dWMS* locking or *PS* locking technique.

4.3.1 Setup

A simplistic schematic of *two-line atomic fluorescence thermometry* setup is shown in *Figure 24*. The setup consists of two diode lasers. A *TOPTICA DL 100 pro design* tunable diode laser is used to sweep the *410 nm* range with the maximum power of *13 mW* and a *TOPTICA DL 110* tunable diode laser with the maximum power of *15 mW* is used to scan the *451 nm* range of frequency. Technical information for *TOPTICA* tunable diode lasers is available on the *TOPTICA OPTICS* website [2]. Two *TOPTICA DC 110 supply and control rack* are used to control the lasers [2].

A dichroic mirror is used to overlap the two laser beams; the mirror transmits wavelengths in a range of *451 nm* and reflects wavelengths in a close interval around *410 nm*. A beam splitter divides the laser beam into two branches, one is used for the frequency stabilization process and the other is used for the *LIF* thermometry. Optical elements of *dWMS* locking setup and *PS* locking setup are explained before.

The National Instrument data acquisition (*DAQ*) card, *NI USB-6363*, is used to communicate with the diode lasers supply and control racks and a photodiode detector [3]. A *Heraeus Noblelight 37 mm* hollow cathode lamp with the maximum current of *10 mA* is used as an indium atom source [4].

A L_1 concave lens with the focal length of *100 mm* and a convex lens L_2 with the focal length of *300 mm* are used to produce a thin sheet of the laser light focused on the burner. Indium atoms are seeded by a seeder designed by Whiddon et al [23], where

tri-methyl-indium (*TMI*) molecules from a bubbler are mixed with combustible gases, producing free indium atoms in the flame. Tri-methyl-indium atoms are seeded by a nitrogen flow to a jet flame. The volumetric flow rate of the seeding nitrogen is $0.2\ ^{lit}/_{min}$, which is approximately equal to *1 ppm* indium atoms concentration in the flame. A collective lens of L_c collects the fluorescence signal to the *CCD* camera used as detector$_2$.

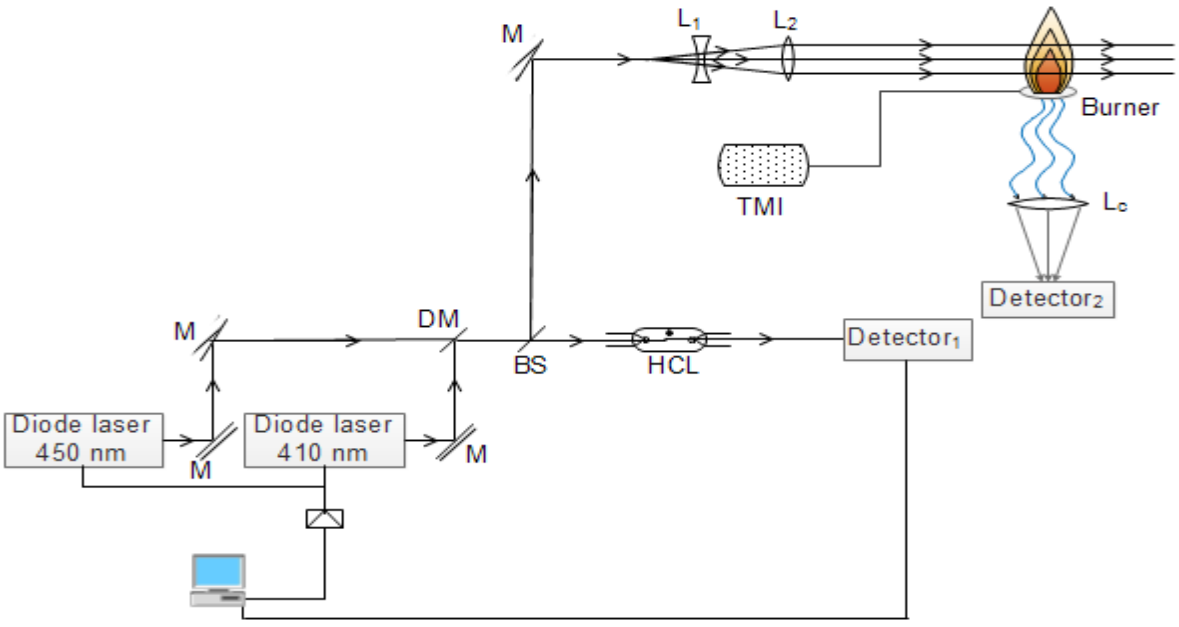

Figure 24 A simple schematic of TLAF thermometry setup, the 410 nm and 451 nm diode lasers are used to excite indium atoms, a dichroic mirror (DM) reflects the 410 nm wavelength and transmits the 451 nm wavelength, a HCL is used as a source of indium atoms for the locking part, a photodiode (detectir$_1$) records the dWMS or PS signal, a beam splitter (BS) separates the laser into two beams, one is used in frequency stabilization and the other is used in TLAF thermometry, L_1 and L_2 lenses are used to produce a thin laser sheet over the burner, tri-methyl-indium molecules are seeded into the burner as a indium atom source, the collective lens, L_c, collects the LIF signals, a CCD camera (detector$_2$) is taking a 2D image of the fluorescence.

A Princeton Instruments *PI-MAX 3 CCD* camera with a *451 nm* band pass filter is used to take two dimensional pictures of the flame, the F-number of the *CCD* camera is *1.4*, ($F_{\#} = 1.4$). Technical information about the camera is available in Princeton Instruments website[5].

A jet flame seeded with indium atoms is used to show the applicability of the temperature measurement technique in laminar flames. The flame is surrounded with a McKenna flat flame co-flow to stabilize the jet flame. *Figure 25* shows the *PS* locking setup along with the burner used in the temperature measurement.

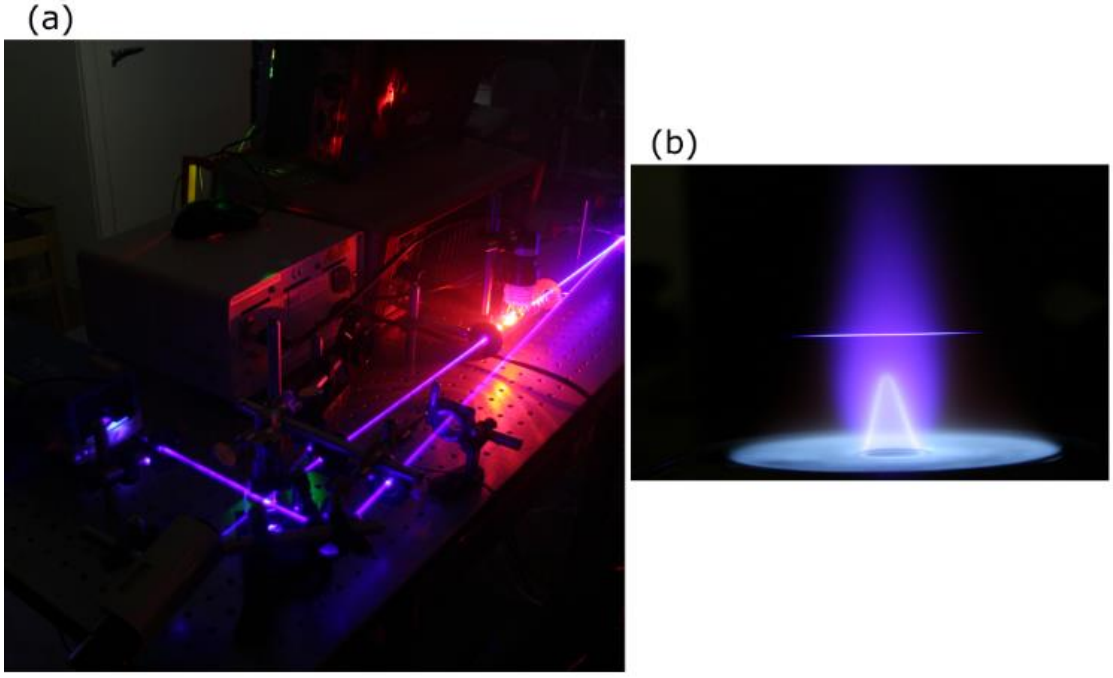

Figure 25 (a) The pictures of the polarization spectroscopy setup used in laser stabilization, (b) the laser light passing through the burner.

4.3.2 Temperature measurement process

A fuel equivalence ratio, $\phi = 0.9$, is used for the co-flow and, $\phi = 1$, for the jet flame. The fuel equivalence ratio, ϕ is defined as the actual fuel to oxidizer ratio to the stoichiometric fuel to oxidizer ratio.

$$\phi = \frac{m_{fuel}/m_{ox}}{\left(m_{fuel}/m_{ox}\right)_{st}} \tag{31}$$

A *CCD* camera with *1024* × *1024* pixels resolution is used for recording the fluorescence signals. The *CCD* camera specifications are: exposure time of *10 μs*, *on-CCD* accumulation of *50* and each picture is averaged over *5* frames. A trigger signal is sent to the *CCD* camera by the *LabVIEW* program every *100 ms* in the locking periods.

The modified *TLAF* thermometry technique is used in the experiments, so a band-pass filter for *451 nm* is used in front of the camera. The *410 nm* and *451 nm*, laser profiles are shown in *Figure 26 (a)* and *Figure 26 (b)*, respectively.

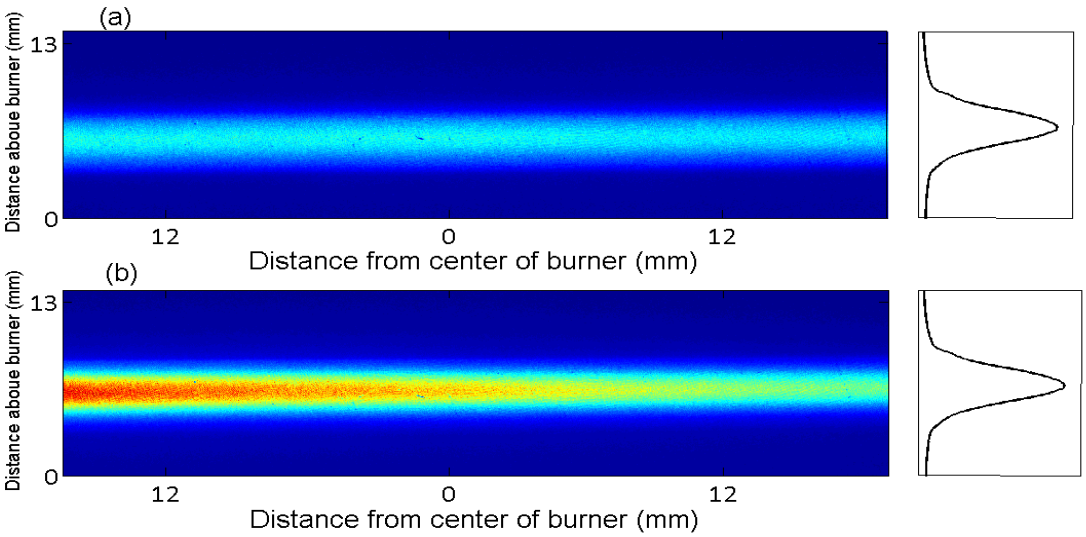

Figure 26 (a) The 410 nm laser profile, (b) the 451 nm laser profile.

The laser profiles are measured by detecting the phosphorescence emissions of the lasers trough a liquid solution of yellow marker Pyranine dye. The normalized laser profiles are used to convert laser powers into intensities.

The *410 nm* and *451 nm* laser powers are measured at the flame and are equal to: P_a *=3.35 mW,* and P_b *= 1.19 mW,* respectively.

Figure 27 (a) shows the Stokes *LIF* signal for the *410 nm* laser denoted in modified *LIF* thermometry technique as F_a. The resonance *LIF* signal for the *451 nm* laser wavelength denoted in modified *LIF* thermometry technique as F_b is shown in *Figure 27 (b).* The intensity of the anti-Stokes fluorescence is almost ten times higher than the intensity of the resonant fluorescence of level |3⟩ in indium atoms.

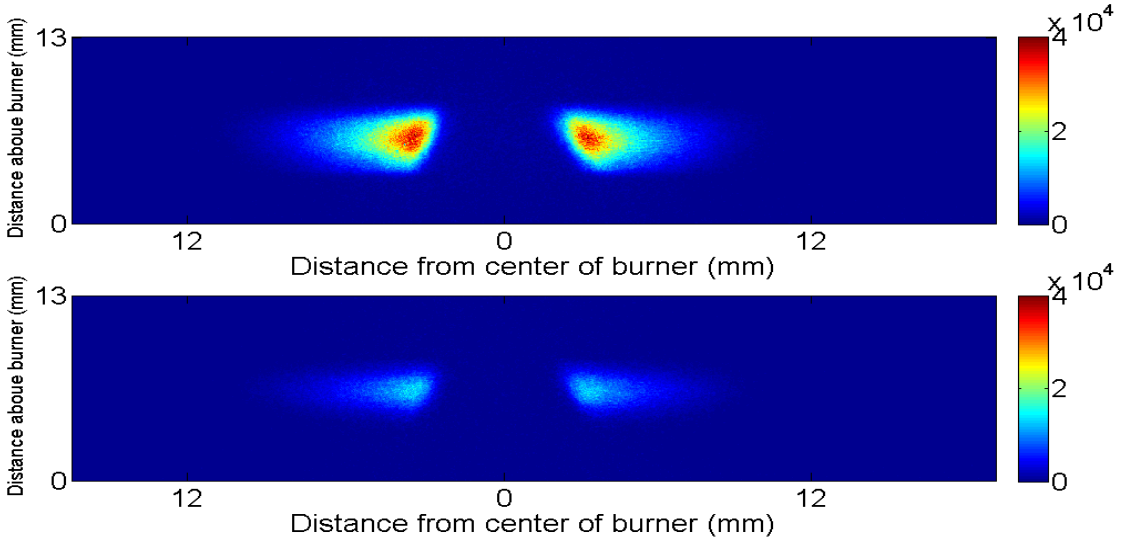

Figure 27 (a) The F_a fluorescence, and (b) the F_b fluorescence signals of indium atoms in the flame.

Equation 30 is used to determine the temperature in the flame by using the modified *TLAF* thermometry technique. *Figure 28* shows the temperature in different

parts of the flame within the laser sheet. The zeros or values close to zero, produced by subtraction of background signal from the *TLAF* signal, are the main reason for the existence of dark dots far from the laser sheet as these values on denominator produce infinity or very large numbers seen as dark dots (high values) in *Figure 28 (a)*. In *Figure 28 (b)* pixels with a value of infinity or values greater than *100000* are set to zero.

Difficulty in alignment of two lasers is one of the major concerns of *TLAF* thermometry. All calculations are based on an assumption that the *410 nm* and *451 nm* laser sheets are exactly overlapping in the flame. As we used the same optical elements to produce a thin sheet of laser, the identical laser profiles and beam waits of diode lasers is essential.

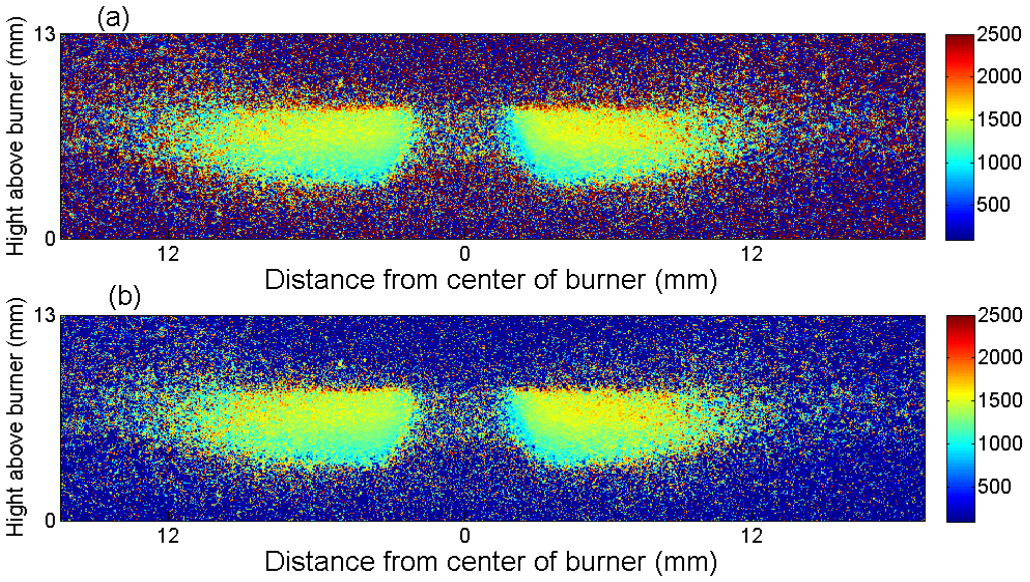

Figure 28 (a) Temperature in the flame for $C_2 = P_a / P_b$, (b) values greater than 100000 in (a) are set to zero.

For accurate temperature measurements the calibration constant C_2 is needed to be measured experimentally. The correction for different detector response to the laser λ_{13}

and λ_{23} power is included in C_2 constant. In the absence of a standard calibration method, the calibration constant has been chosen to be equal to the ratio of P_a *to* P_b. Normally the temperature calibration in a flame is done by a *coherent anti-Stokes Raman scattering spectroscopy* as a standard technique.

To investigate the precision of the measurements the relative errors defined as:

$$RE_i = \frac{(F_a)_i - (F_a)_{i+1}}{(F_a)_i} \tag{32}$$

is used to compare laser induced fluorescence images acquired at different times. The subscripts, *i* and *i+1*, denote two consecutive measurements and the relative error *RE* gives an indication of the reproducibility and precision of the measurement. In Figure 29 the relative errors of the two lasers are shown for three different measurements.

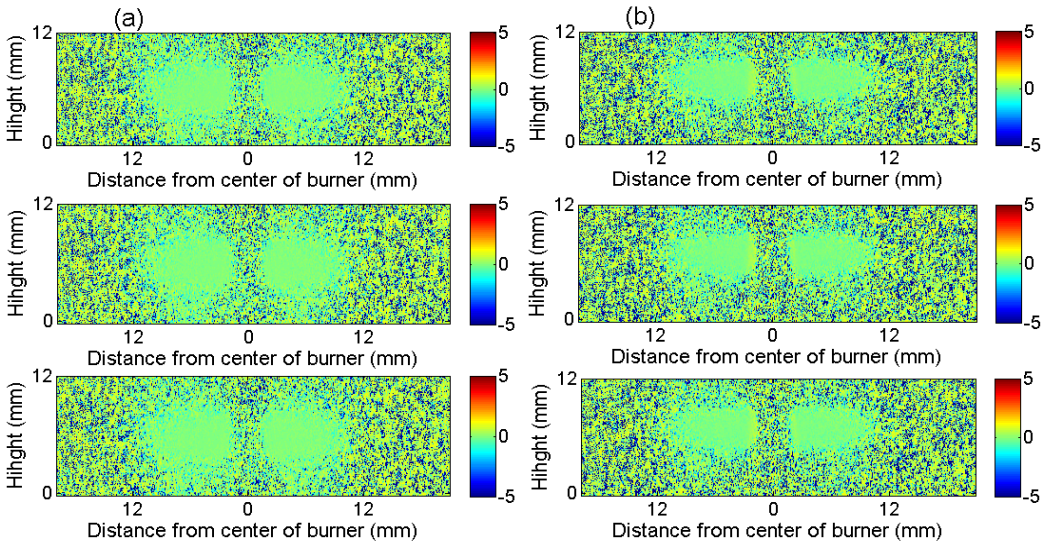

Figure 29 (a) Relative errors of F_a , for four consecutive measurements, (b) relative errors of F_b, for four consecutive measurements.

The mean relative error of F_a within the laser sheet is -6.7×10^{-04}. The mean relative error of F_b within the laser sheets is -4.5×10^{-04}. The low relative error is an

indication of high repeatability of measurements. The relative error of F_a / F_b propagates to the evaluation of the *TLAF* temperature.

Uncertainty in locking the laser to the exact transition of the indium atoms is another source of error in *TLAF* temperature measurements. *Figure 30* shows the simulated line shapes of *410 nm* and *451 nm* transitions of indium atoms, for *1500° K* and *1 atm* pressure compared to the line shapes of indium atoms in the low pressure hollow cathode lamp.

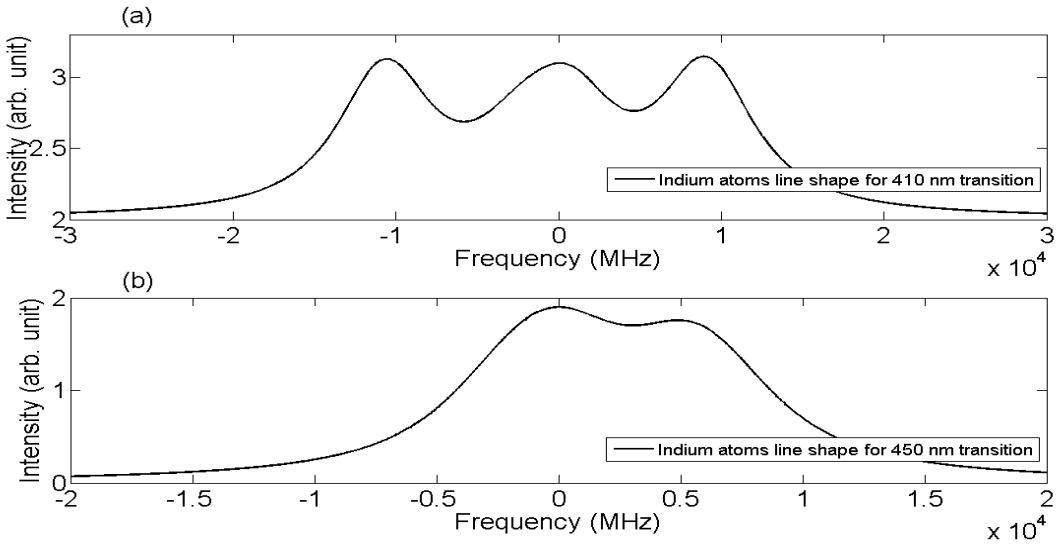

Figure 30 The simulated line shape of indium atoms for (a) 410 nm transitions, and (b) 451 nm transitions in the room pressure.

For the worst case the laser is locked within *715 MHz* of the transition for *dWMS* laser locking method with constant modulation amplitude. The *715 MHz* uncertainty in frequency locking is equal to maximum *0.64%* error in measuring the intensity for *410 nm* indium transitions and maximum error of *2.00%* in intensity measurement of *451 nm* transitions. The lowest locking frequency interval is *110 MHz* and is equal to

maximum errors of *0.065%* and *0.053%* in measuring the intensity of *410 nm* and *451 nm* transitions, respectively.

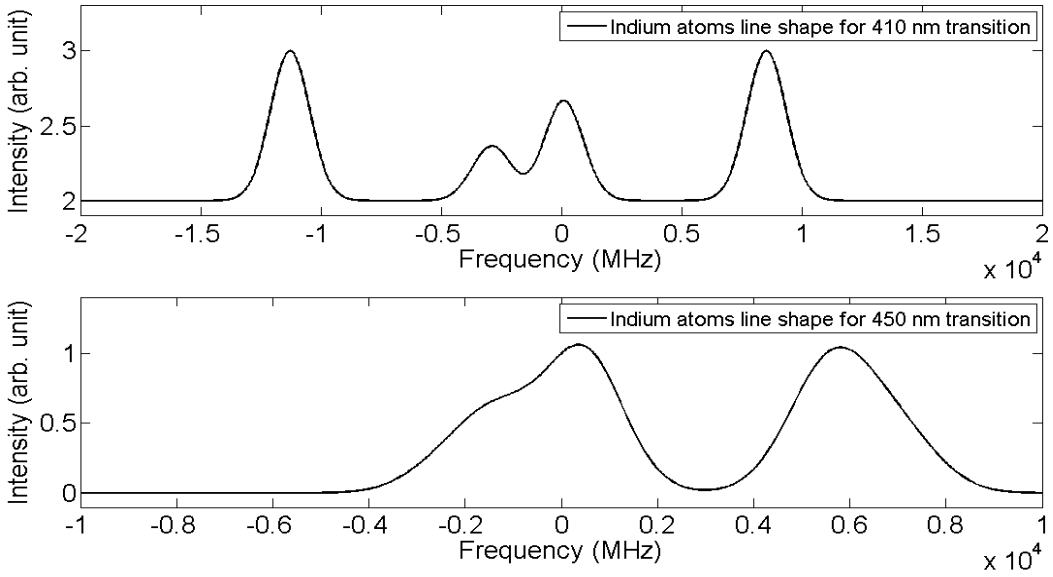

Figure 31 The simulated line shape of indium atoms for (a) 410 nm transitions, and (b) 451 nm transitions for the HCL pressure.

The pressure inside *HCL* is much lower than *1 atm* (6.58×10^{-3} *atm*) so the transition peaks are much narrower (*Figure 31*); the narrower peaks increase the accuracy of locking the laser to atomic transitions.

Different methods of tunable diode laser frequency stabilization e.g. *Zeeman shift* [24], *wavelength modulation spectroscopy* [25], and *Doppler free saturation spectroscopy* [26] are discussed in the literatures. The objective of the locking techniques is to minimize diode lasers *FWHM* around the resonant atomic transition. The *FWHM* of different stabilization techniques varies from several hundred megahertz for wavelength modulation and Zeeman shift methods to a few megahertz for Doppler free techniques

such as *saturation spectroscopy* and *polarization spectroscopy*. Higher *FWHM* of *PS* locking technique employed in this thesis in comparison with the Doppler free stabilization technique discussed in the reference [26] is caused by employing a diode laser external cavity and a detector with lower resolutions in the locking setup. However the *FWHM* of indium atoms absorption peak in the room pressure (in order of gigahertz) used in modified *TLAF* thermometry technique is much higher than the stabilized diode laser bandwidth (in order of megahertz) and causes a negligible error in experiments.

The measurement precision of modified *TLAF* thermometry of indium atoms for *451 nm LIF* in this thesis (less than *0.1%*) is far higher than the precision of well stablished thermometry techniques, like *CARS*, Raman scattering (*1-2%*, *2%*, respectively) [1] in the laminar flame as well as the precision *TLAF* thermometry technique (*2.5%*) discussed in the reference [22]. The high precision of the measurements is the result of stable laser sources as well as advantages of seeding the indium molecules in gaseous form to the laminar flame.

5. Conclusions

Frequency stabilization of a diode laser by *digital wavelength modulation spectroscopy* and *polarization spectroscopy* techniques has been successfully performed in this thesis work and applied in two-line atomic fluorescence flame thermometry.

An indium hollow cathode lamp produces a gaseous sample of indium atoms that is used for laser probing. Two spectroscopic methods have been used to lock tunable diode lasers to transitions of indium. The *dWMS* locking technique generates a modulated signal, demodulation of *dWMS* signal produces different harmonics that can used as background free error signals with good signal to noise ratio for the locking process. The *dWMS* locking program reduces the scanning and modulation amplitude of the modulated signal and tries to minimize the fitting residual of a quadratic function to the second harmonic. It has been observed that the *dWMS* can stabilize the diode laser frequency inside a short *250 MHz* interval around the transition frequency.

The *PS* locking technique uses a periodic approach. A short time period is used to scan the laser and find the frequency of the indium atom's transition; after that in a rather long locking period, the laser frequency is set to the indium atoms transition's frequency. For *PS* the laser frequency has been stabilized inside a short frequency interval of *120 MHz*.

Indium atoms in *HCL* have been generated in a low pressure environment. Narrow transition peak, due to low pressure broadening, improves the accuracy of frequency stabilization in either technique.

The *TLAF* thermometry has been chosen as an example of frequency stabilized diode laser. The *TLAF* thermometry has been chosen because of its advantages over *LIF*

thermometry. No need for collisional quenching calculation and high transitions is some examples of its advantages.

Furthermore, the experimental results have shown a high repeatability. The mean relative error of temperature measurements are in 10^{-4} order, promises high precision temperature measurements.

Even though the experimental results are promising, there is room for improvements. The *dWMS* locking technique could be further improved by increasing the modulation frequency, also a better fitting function reduces the scanning frequency interval, moving the fitting to higher harmonics, i.e. fourth or sixth harmonic improve the accuracy of the laser. The *dWMS* locking technique could also be performed periodically, the inflection points of odd harmonics and the maxima and minima of even harmonics correspond to the resonant frequency of transitions. The advantage of using a periodic technique is that the laser is unmodulated during a measurement, except error in finding an exact transition point the only limiting factor of frequency stabilization is diode lasers or external cavities bandwidth. Production of more stable diode lasers with higher intensities would reduce the frequency stabilization range dramatically.

Popular summary

At a first glance stabilized continuous wave laser seems to have no use in everyday life, but its application in technologies like the global positioning system (*GPS*) is an essential part of modern life. Continuous wave lasers are also widely used in many different spectroscopic techniques; make it possible to analyze the material in order to improve our understanding of the surrounding environment. By choosing the correct color of the laser t specific species can be made to emit fluorescence signals, these fluorescence signal may be used as a fingerprint to detect the specie or measure the characteristics of the specific specie. The wavelength required for an atom to be excited is called a transition wavelength. By stabilizing the laser to an atomic transition wavelength the resulting fluorescence can be continuously monitored.

In this thesis two spectroscopic methods are used to stabilize tunable diode lasers to transitions of indium atoms, wavelength modulation spectroscopy and polarization spectroscopy. The source of indium atoms used for frequency stabilization is a hollow cathode lamp. Hollow cathode lamp produces indium atoms in a low pressure environment so indium atoms are less likely to collide with each other or the container surface. Depending on the amount of exchanged energy by collisions; atoms absorb or emit different frequencies. Low pressure environment reduces the atom collisions therefore reduces the variation in the absorbed or emitted frequency of atoms.

The wavelength modulation spectroscopy technique is a variation of absorption spectroscopy with higher signal to noise ratio compare to the normal absorption spectroscopy. The wavelength modulation spectroscopy frequency stabilization technique stabilizes the diode laser frequency in a range of several hundred megahertz around the absorption frequency of transition.

Polarization spectroscopy is another technique used in this thesis to stabilize tunable diode lasers. Indium atoms in gaseous form travel randomly in the space. The light source frequency observed by an atom is relative to the velocity and the direction of atom movement. When an atom moves toward a light source each successive wave maxima or minima to reach the atom in a slightly shorter time compared to a stationary atom, so the light source frequency observed by a moving atom is higher compared to the light source frequency observed by a stationary atom, vice versa atoms moving away from the light source observe lower light frequency compared to stationary atoms. In the polarization spectroscopy technique only stationary atoms contribute to the signal, so atoms moving toward a light source or away from it do not broaden the signal. Without this broadening the diode laser is stabilized in a shorter range compared to the wavelength modulation spectroscopy. The stabilization interval for this technique is dozens of megahertz around the resonant transition frequency. The stabilized lasers are used to excite indium atoms introduced in a flame for temperature measurements.

Combustion processes play a major role in modern civilization as around 80% of today's energy come from fossil fuels. From energy conversion to simple burners used for heating, combustion is present in everyday life. Knowing the temperature throughout a combustion system helps to understand the chemical reaction and species of the system and facilitate the improvements of the processes.

The temperature in a flame is calculated by measuring the fluorescence signals in the flame. Fluorescence is a spontaneous emission of light from an excited electronic state. In laser induced fluorescence, laser light is used to excite a population of a lower level to an excited state. The stabilized diode lasers described in the first part of this thesis are used to excite atoms. The energy gained from the laser absorption makes the atoms unstable; the unstable atoms then lose the excess energy by collisions, ionization,

dissociation or emitting the light that is called fluorescence. The intensity of a fluorescence signal is a function of the initial population of the levels. The population of levels in an atom only depends on the temperature; therefore the fluorescence signal intensity emitted by an atom is proportional to the temperature of the atom.

Two-line atomic fluorescence (*TLAF*) is used in the thesis to measure the temperature. *TLAF* thermometry utilizes the ratio of two fluorescence signals excited from two different lower levels to a common upper level to measure the temperature. In this thesis indium atoms are used for the *TLAF* thermometry. A *2D* temperature map of a flame is taken by the *TLAF* thermometry technique.

Self-reflection

During the year that I have been working on my master thesis, I acquired experience and knowledge which I consider very important for my personal evolution and my professional career. By my supervisors' guidance I have learnt how to work in an extended project and how to overcome different problems that I have faced in my work. I gained confidence to handle more advanced scientific questions and learnt how to overcome the difficulties of a project by studying more deeply to get a profound understanding of the problem. The most important realization from my work during this year; I consider to be the experience that I have gained on finding a theoretical solution for a problem and applying it in the laboratory and analyzing the results. I learnt how to divide a complex problem into smaller parts and after solving these parts how to integrate these solutions in order to obtain a total solution. By my supervisors' help I have learned about planning an experiment. Presenting my result orally and in a written form helped me improve my scientific writing and communication skills.

Furthermore, the knowledge that I acquired in the two different areas of spectroscopy and combustion is very important. I have learnt how to apply a spectroscopic method in a combustion system in order to measure a characteristic of it. I have used digital wavelength modulation spectroscopy and polarization spectroscopy to stabilize a diode laser and after that I have applied the stabilized laser in two-line atomic fluorescence thermometry to measure the temperature of a combustion system. I have learned how to build a spectroscopic setup, how to align the laser beam and use different optical elements.

Finally, I gained experience in computer programming and signal processing, I have learnt how to write continuous and complex programs in *LabVIEW* and *Matlab*

software, how to use data acquisition in these programs and how to process signals by using the Fourier method and filtering.

Acknowledgements

I would like to thank my supervisors Prof. Zhongshan Li and Jesper Borggren for giving me the chance to work in this very interesting subject. They were always very supportive and willing to answer every question and help with every problem. They taught me how to work in an extended project and I have acquired important experiences and knowledge during this one year that he supervised my thesis.

Finally, I would like to thank all my friends for their support.

BIBLIOGRAPHY

[1] A. Eckbreth, Laser Diagnostics for Combustion Temperature and Species, Gordon adn Breack Publishers, 1996.

[2] P. Lundin, "Laser Sensing for Quality Control and Classification," Lund University, 2014.

[3] K. Duffin, A. McGettrick, W. Johnstone, G. Stewart and D. Moodie, "Tunable Diode-Laser Spectroscopy with Wavelength Modulation: a Calibration-Free Approach to the Recovery of Absolute Gas Absorption Line Shapes," *Journal of Lightwave Technology,* vol. 25, no. 10, pp. 3114-3125, 2007.

[4] D. Luss and N. Brauner, "Tunable Diode Laser Absorption Spectroscopy (TDLAS) in the Process Industries – a Review," *Reviews in Chemical Engineering,* vol. 23, no. 2, Apr 2007.

[5] G. Rieker, "Calibration-Free Wavelength-Modulation Spectroscopy for Measurements of Gas Temperature and Concentration in Harsh Environments," *Applied optics,* vol. 48, no. 29, pp. 5546-5560, 10 Oct.09.

[6] K. Ruxtona, A. Chakrabortya, W. Johnstonea, M. Lengdena, G. Stewarta and K. Duffinb, "Tunable Diode Laser Spectroscopy with Wavelength Modulation: Elimination of Residual Amplitude Modulation in a Phasor Decomposition Approach," *Sensors and Actuators B: Chemical,* vol. 150, no. 1, p. 367–375, 2010.

[7] J. Henningsen and H. Simonsen, "Quantitative Wavelength-Modulation Spectroscopy without Certified Gas Mixtures," *Applied Physics B,* vol. 70, no. 4, pp. 627-633, April 2000.

[8] D. Bomse, A. Stanton and J. Silver, "Frequency Modulation and Wavelength Modulation Spectroscopies: Comparison of Experimental Methods Using a Lead-Salt Diode Laser," *Applied Optics,* vol. 31, no. 6, p. 718:731, 20 Feb. 1992.

[9] J. Supplee, E. Whittaker and W. Lenth, "Theoretical Description of Frequency Modulation and Wavelength Modulation Spectroscopy," *Applied Optics,* vol. 33, no. 27, 20 Sep. 1994.

[10] J. Reid and D. Labrie, "Second-Harmonic Detection with Tunable Diode Lasers," *Applied Physics B,* vol. 26, no. 3, pp. 203-210, Nov. 1981.

[11] "TOPTICA PHOTONICS," [Online]. Available: http://www.toptica.com/products. [Accessed June 2015].

[12] "National Instruments," [Online]. Available: http://www.ni.com/. [Accessed June 2015].

[13] "Heraeus Noblelight," [Online]. Available: http://www.heraeus-noblelight.com/en/hollow_cathode_lamp_finder.aspx. [Accessed June 2015].

[14] D. Wolfgang, Laser Spectroscopy 2, Experimental Techniques, 5th Edition, Springer, 2015.

[15] C. Bohren, "What did Kramers and Kronig do and how did they do it?," *European Journal of Physics,* vol. 31, no. 3, p. 573–577, 2010.

[16] D. Preston, "Doppler-Free Saturated Absorption: Laser Spectroscopy," *Journal of American Physics,* vol. 64, pp. 1432-143664, 1996.

[17] V. Stert and R. Fischer, "Doppler-Free Polarization Spectroscopy Using Linear Polarized Light," *Applied physics,* vol. 17, no. 2, pp. 151-154, 1978.

[18] A. Hall and R. Eckberth, "CARS Thermometry in a Sooting Flame," *Combustion and Flame,* vol. 36, pp. 87-98, 1979.

[19] G. Elliott, NGlumac and C. Carter, "Molecular Filtered Rayleigh Scattering Applied to Combustion," *Measurement Science and Technology,* vol. 12, no. 4, p. 452–466, 2001.

[20] J. Engström, J. Nygren, M. Aldén and C. Kaminski, "Two-Line Atomic Fluorescence as a Temperature Probe for Highly Sooting Falmes," *Optics Letters,* vol. 25, no. 19, 1 Oct. 2000.

[21] R. Joklik and J. Daily, "Two-Line Atomic Fluorescence Temperature Measurement in Flames: an Experimental Study," *Applied optics,* vol. 21, no. 22, 15 Nov. 1982.

[22] J. Hult, I. Burns and C. Kaminski, "Two-Line Atomic Fluorescence Flame Thermometry Using Diode Lasers," *Proceedings of the Combustion Institute 30,* vol. 30, p. 1535–1543, 2005.

[23] R. Whiddon, B. Zhou, J. Borggren, M. Aldén and Z. Li, "Vapor Phase Tri-methyl-indium Seeding System Suitable for High Temperature Spectroscopy and Thermometry," *Under review for (Review of Scientific Instrument) Journal.*

[24] K. Corwin, Z. Lu, C. Hand, R. Epstein and C. Wieman, "Frequency-Stabilized Diode Laser with the Zeeman Shift in an Atomic Vapor," *Applied Optics,* vol. 37, no. 15, 20 May 1998.

[25] K. Numata, J. Chen, S. Wu, J. Abshire and M. Krainak, "Frequency Stabilization Of Distributed-Feedback Laser Diodes at 1572 nm for Lidar Measurements of Atmospheric Carbon Dioxide," *Applied Optics,* vol. 50, no. 7, 1 Mar. 2011.

[26] J. Smith, X. Chu, W. Huang and J. Wiig, "Labview-Based Laser Frequency Stabilization System with Phase-Sensitive Detection Servo Loop for Doppler Lidar Applications," *Optical Engineering,* vol. 47, no. 11, Nov. 2008.

[27] "Princeton Instruments," [Online]. Available: http://www.princetoninstruments.com/. [Accessed June 2015].

[28] M. O'Callaghan and J. Cooper, "Theory of Velocity-Dependent, Collision-Broadened, Doppler-Free Line Shapes," *Physical Review A,* vol. 39, no. 12, 15 Jun 1989.

[29] K. MacAdam, A. Steinbach and C. Wieman, "Narrow Band Tunable Diode Laser System with Grating Feedback, and a Saturated Absorption Spectrometer for Cs and Rb," *American Journal of Physics,* vol. 60, pp. 1098-1111, 1992.